Protein Synthesis, Post-Translation Modification, and Degradation:

Oxidative Stress Induces Nuclear Loss of DNA Repair Proteins Ku70 and Ku80 and Apoptosis in Pancreatic Acinar AR42J Cells

Ji Yeon Song, Joo Weon Lim, Hyeyoung Kim, Tomohiro Morio and Kyung Hwan Kim

J. Biol. Chem. 2003, 278:36676-36687.
doi: 10.1074/jbc.M303692200 originally published online July 16, 2003

THE JOURNAL OF BIOLOGICAL CHEMISTRY
Vol. 278, No. 38, Issue of September 19, pp. 36676–36687, 2003
Printed in U.S.A.

Oxidative Stress Induces Nuclear Loss of DNA Repair Proteins Ku70 and Ku80 and Apoptosis in Pancreatic Acinar AR42J Cells*

Received for publication, April 9, 2003, and in revised form, July 14, 2003
Published, JBC Papers in Press, July 16, 2003, DOI 10.1074/jbc.M303692200

Ji Yeon Song‡, Joo Weon Lim‡, Hyeyoung Kim‡§, Tomohiro Morio¶, and Kyung Hwan Kim‡

From the ‡Department of Pharmacology and Institute of Gastroenterology, Brain Korea 21 Project for Medical Science, Yonsei University College of Medicine, Seoul 120-752, Korea and the ¶Department of General Medicine, Tokyo Medical and Dental University School of Medicine, Tokyo 113-8519, Japan

Cell death linked to oxidative DNA damage has been implicated in acute pancreatitis. The severe DNA damage, which is beyond the capacity of the DNA repair proteins, triggers apoptosis. It has been hypothesized that oxidative stress may induce a decrease in the Ku70 and Ku80 levels and apoptosis in pancreatic acinar cells. In this study, it was found that oxidative stress caused by glucose oxidase (GO) acting on β-D-glucose, glucose/glucose oxidase (G/GO), induced slight changes in cytoplasmic Ku70 and Ku80 but drastically induced a decrease in nuclear Ku70 and Ku80 both time- and concentration-dependently in AR42J cells. G/GO induced apoptosis determined by poly(ADP-ribose) polymerase cleavage, an increase in expression of p53 and Bax, and a decrease in Bcl-2 expression. G/GO-induced apoptosis was in parallel with the loss of nuclear Ku proteins in AR42J cells. Caspase-3 inhibitor prevented G/GO-induced nuclear Ku loss and cell death. G/GO did not induce apoptosis in the cells transfected with either the Ku70 or Ku80 expression gene but increased apoptosis in those transfected with the Ku dominant negative mutant. Pulse and pulse-chase results show that G/GO induced Ku70 and Ku80 syntheses, even though Ku70 and Ku80 were degraded both in cytoplasm and nucleus. G/GO-induced decrease in Ku binding to importin α and importin β reflects possible modification of nuclear import of Ku proteins. The importin β level was not changed by G/GO. These results demonstrate that nuclear decrease in Ku70 and Ku80 may result from the decrease in Ku binding to nuclear transporter importins and the degradation of Ku proteins. The nuclear loss of Ku proteins may underlie the mechanism of apoptosis in pancreatic acinar cells after oxidative stress.

Oxidative stress is regarded as a major pathogenic factor in acute pancreatitis (1). This hypothesis was demonstrated by the high levels of lipid peroxide, which is an index of oxidative membrane damage, in the serum of the patients with acute pancreatitis (2). Scavenger therapy for reactive oxygen species (ROS)[1] has attained some success in experimental pancreatitis models (1, 3, 4). In human acute pancreatitis, the increased levels of lipid peroxidation products in the bile or pancreatic tissue (5–7) and the subnormal levels of antioxidant vitamins in the blood (8, 9) have been reported. Once produced, ROS can act as a molecular trigger for various inflammatory processes. They can attack the biological membranes directly and trigger the accumulation of neutrophils (10) and their adherence to the capillary wall (11). Therefore, it is probable that ROS play a central role in perpetuating the pancreatic inflammation and the development of extrapancreatic complications (12).

Inflammation and acinar cell death are the hallmarks of both human and experimental pancreatitis (13, 14). Although significant progress in understanding the inflammatory response has been achieved over the past decade, the mechanisms of acinar cell death in pancreatitis remain largely unexplored. In pancreatitis, acinar cell death occurs by both necrosis and apoptosis (15–18). Apoptosis is a programmed form of cell death that is characterized by a series of distinct morphological and biochemical changes including the condensation of nuclear chromatin and DNA fragmentation that occurs in response to a variety of stress-related stimuli (19, 20). One report suggested that severe forms of acute pancreatitis involve primarily necrosis, whereas the mild forms predominantly involve apoptosis and marginal amounts of necrosis of the exocrine pancreatitis (18). Recent studies have revealed that apoptosis is a major mechanism of acinar cell death in various experimental models of acute pancreatitis, suggesting a role for apoptosis in the pathophysiology of the disease (21, 22). The molecular mechanisms responsible for apoptosis in pancreatic acinar cells remain to be defined.

The Ku70 (70 kDa) and Ku80 (80 kDa) proteins are DNA-binding regulatory subunits of DNA-dependent protein kinase (DNA-PK) that are composed of a 470-kDa catalytic subunit (DNA-PKcs) and Ku proteins (23, 24). The Ku70 and Ku80 proteins act as the regulatory parts of the DNA-PK and initiate the repair process of DNA double-stranded breaks, which produce DNA fragmentation, by activating DNA-PK after binding to the DNA double-stranded breaks (23). In addition to the regulatory function of the Ku proteins in DNA-PK, heterodimers of both Ku70 and Ku80 also have independent DNA repair functions. These include single-stranded DNA-dependent ATPase activity and the binding and repair of broken single-stranded DNA, single-stranded nicks, gaps in DNA, and single-stranded to double-stranded transitions in DNA (23, 24). Oxidative damage to nucleic acids can produce adducts of the base residues and sugar residues, which may lead to the generation of single-stranded breaks. Less frequently, oxidation

* This study was supported by a grant from the Korean Ministry of Health and Welfare (to H. K.). The costs of publication of this article were defrayed in part by the payment of page charges. This article must therefore be hereby marked "*advertisement*" in accordance with 18 U.S.C. Section 1734 solely to indicate this fact.

§ To whom correspondence should be addressed. Tel.: 82-2-361-5232; Fax: 8-2-313-1894; E-mail: kim626@yumc.yonsei.ac.kr.

[1] The abbreviations used are: ROS, reactive oxygen species; GO, glucose oxidase; G/GO, glucose/glucose oxidase; DNA-PK, DNA-dependent protein kinase; MTT, 3-(4,5-dimethylthiazol-2-yl)-2,5-diphenyltetrazolium bromide; GST, glutathione *S*-transferase; NLS, nuclear localization signal; PARP, poly(ADP-ribose) polymerase; DAPI, 4′,6′-diamidino-2-phenylindole; Z, benzyloxycarbonyl; fmk, fluoromethyl ketone; PBS, phosphate-buffered saline; DTT, dithiothreitol; DMEM, Dulbecco's modified Eagle's medium.

can cause cross-links to other molecules and double-stranded breaks (25). Oxidative injury caused by ischemia/reperfusion in the rabbit spinal cord induces reversible neurological deficits with increased Ku-DNA binding activity, which is an indicator of a DNA-PK activation, whereas severe ischemia/reperfusion causes permanent deficits that are accompanied by decease in the Ku-DNA binding activity. This suggests that Ku has a defensive role against oxidative injury (26). Embryo fibroblasts derived from Ku80-null (Ku80−/−) mice were more susceptible to H_2O_2-triggered DNA damage than those from the wild-type mice (27). Therefore, it is assumed that Ku may play a role in the cell death mechanisms, particularly DNA fragmentation after oxidative stress, and that Ku reduction may involve the mechanism of apoptotic cell death.

Several protease families are implicated in apoptosis, the most prominent being caspase (28). Caspases are cysteine-containing, aspartic acid-specific proteases that exist as zymogens in the soluble cytoplasm, the mitochondrial intermembrane space, and the nuclear matrix of virtually all cells (29). Upon activation, the caspases cleave numerous cellular proteins, including poly(ADP-ribose) polymerase (PARP) (29). In fact, almost 100 cellular proteins have now been identified as potential caspase substrates during apoptosis, and most events in apoptosis appear to require a caspase-mediated proteolytic process (30). The 460-kDa catalytic subunit of DNA-PK is also substrate for caspase-3, which is activated by ischemia/reperfusion (26) and ROS (31–36). The reduction in the Ku-DNA binding activity (which is critical to DNA PK activation) after prolonged ischemia, which is accompanied by a reduction in the Ku protein and the proteolysis of PARP, suggests that a reduction in Ku might be involved downstream from the caspase-activating apoptotic pathway after ischemia/reperfusion (26). Moreover, four nucleoporins, Nup153, RanBP2, Nup214, and Tpr are cleaved by caspases during apoptosis (37). Nuclear transport factors, Ran, importin α, and importin β are not proteolytically processed but redistribute across the nuclear envelope independently and prior to caspase activation (37). Macromolecules with a molecular mass greater than 40–60 kDa enter the nucleus via active transport (38). This transport route requires an adaptor protein, importin α, that links the nuclear cargo to importin β. This classical nuclear protein import requires energy, soluble transport factors, and nuclear localization sequences (NLSs), specialized signals that target proteins into the nucleus. In classical nuclear transport, these signals can be of two types: monopartite or bipartite. Monopartite signals are simple stretches of basic amino acids, whereas bipartite NLSs contain two clusters of basic amino acids separated by a spacer region (39). The structure of the Ku70 NLS resembles the consensus of a bipartite-type NLS (40). Both Ku70 NLS and Ku80 NLS are mediated to target to the nuclear rim by two compartments of the nuclear pore-targeting complex, importin α and importin β (40, 41). Because the integrity of the nuclear pore may be essential for nucleocytoplasmic transport, caspase-mediated cleavage of nucleoporins may interfere nuclear translocation of Ku70 and Ku80 during apoptosis. Modifications in the machinery responsible for nucleocytoplasmic transport, such as redistribution of Ran, importin α, and importin β between the nucleus and the cytoplasm, may inhibit nuclear import of Ku proteins during apoptosis.

This study investigates the role of Ku70 and Ku80 on apoptotic cell death, which is induced by oxidative stress in pancreatic acinar AR42J cells. To explore the changes in the Ku proteins in the cell death pathway after oxidative stress, the Ku expression level, cell viability, and apoptosis were determined before and after treatment with H_2O_2. H_2O_2 is continuously generated by glucose oxidase (GO) acting on β-D-glucose, which is expressed as glucose/glucose oxidase (G/GO). To determine the apoptotic cleavage of Ku, Ku expression, the intracellular distribution, and the cell viability were determined in the cells treated with G/GO in the presence or absence of the caspase-3 inhibitor. In addition, the cell viability and DNA fragmentation were compared among the wild-type cells, and the cells transfected with the pcDNA expression vector (pcN-3), the Ku dominant negative mutant (KuD/N), or either the Ku70 or Ku80 expression gene ($Ku70^+$, $Ku80^+$) treated with G/GO. Transfection was confirmed by an increase in Ku expression in the cells transfected with $Ku70^+$ or $Ku80^+$. Functional efficiency was determined by a loss of Ku-DNA binding activity in the cells transfected with KuD/N. As the apoptotic indices, PARP cleavage and the expression changes in p53, Bcl-2, and Bax were monitored in the wild-type cells treated with G/GO. To determine the effect of G/GO on Ku synthesis and degradation, the wild-type cells were pulsed or pulse-chased with [^{35}S]methionine with or without the G/GO treatment and immunoprecipitated with anti-Ku70 or anti-Ku80 antibodies. To determine whether nuclear import of Ku proteins is inhibited by G/GO, *in vitro* binding assay using glutathione *S*-transferase (GST)-importin α fusion protein was performed in the wild-type cells treated with G/GO. The bound protein levels were determined by Western blotting for Ku70, Ku80, and importin β. The importin β level was monitored in the wild-type cells treated with or without G/GO.

EXPERIMENTAL PROCEDURES

Cell Lines and Culture Condition—The rat pancreatic acinar AR42J cells (pancreatoma, ATCC CRL 1492) were obtained from the American Type Culture Collection (Manassas, VA) and cultured in Dulbecco's modified Eagle's medium (Sigma) supplemented with 10% fetal bovine serum (Invitrogen) and antibiotics (100 units/ml penicillin and 100 μg/ml streptomycin).

Plasmid Construction—The human cDNA for Ku70 and Ku80 was derived from human Ku70/pET1a and Ku80/pET1a, respectively. The insert was digested with *Bam*HI and *Eco*RI and subcloned into the *Bam*HI-*Eco*RI sites of the pcDNA3 vector (Invitrogen), which was used for the Ku70 or Ku80 expression plasmid construct (as $Ku70^+$ or $Ku80^+$). A C-terminal human Ku80 (427–732) expression vector was generated by PCR using the Ku80 cDNA vector with a specific set of primers to generate the artificial *Kpn*I and *Bam*HI sites at the 5′ and 3′ ends, respectively. The sequences of the primers used are as follows: 5′-TGCAGGTACCTATCATGGAAGACTTGCG-3′ and 5′-GGTACCTAGGTGCTGGATATAGTACAGG-3′. A *Kpn*I-*Bam*HI fragment of the product was subcloned into the *Kpn*I and *Bam*HI sites of the pcDNA3 vector, which was used for the C-terminal Ku80 (427–732) expression plasmid construct (as KuD/N). The PCR-derived part was confirmed by sequencing analysis. For *in vitro* binding assay, cDNA fragment encoding for the full-length rat importin-α was amplified by PCR and subcloned into the *Bam*HI-*Xho*I site of pGEX-5X-1 (Amersham Biosciences).

Transfection—Subconfluent AR42J cells, plated in a 10-cm culture dish, were transfected with each 10 μg of the pcDNA-3 vector (as pcDNA), the C-terminal Ku80 (427–732) expression plasmid construct (as KuD/N), the Ku70 or Ku80 expression plasmid construct (as $Ku70^+$ or $Ku80^+$) using *N*-[1-(2,3-dioleoyloxy) propyl]-*N*,*N*,*N*-trimethyl ammonium methylsulfate (Roche Applied Science) for 16 h. After transfection, the cells were trypsinized and plated at 3×10^4 cells/10-cm culture dish. The cells were then cultured overnight and treated with or without G/GO (5 milliunits) for 12 h. The cytoplasmic and nuclear extracts were prepared from the cells. The Ku70 and Ku80 protein levels were determined by Western blot analysis (see Fig. 6). The functional efficiency of the C-terminal Ku80 (427–732) expression gene was examined by determining the Ku-DNA binding activity with an electrophoretic mobility shift assay (see Fig. 7). Transfection efficiency of the C-terminal Ku80 (427–732) expression gene using polyclonal antibody for Ku80 could not be determined by Western blot analysis (data not shown) as previously reported (42).

Experimental Protocol—To determine whether H_2O_2 induces apoptosis in pancreatic acinar cells and whether the changes in the Ku proteins are related to acinar cell death, β-D-glucose (10 mM) and GO (5 milliunits/ml) were added to the acinar cells. The wild-type cells and the

cells transfected with either the control pcDNA3 vector (pcN-3) or the C-terminal Ku80 (427–732) expression gene (KuD/N) or the cells transfected with either the Ku70 or Ku80 expression gene ($Ku70^+$ or $Ku80^+$) were used. The Ku-DNA binding activity and Western blotting for Ku70 and Ku80 were used to determine the functional efficiency and the transfection efficiency, respectively. The cells were incubated at 37 °C for 12 h for Western blotting for Ku70 and Ku80 in the whole cell extracts, the cytoplasmic extracts, and the nuclear extracts (see Fig. 6), as well as the Ku-DNA binding activity (see Fig. 7).

To determine the extent of cell viability and apoptosis, the cells were treated with β-D-glucose (10 mM) and GO (3 and 5 milliunits/ml) and cultured for 24 h. The cell viability was determined directly by cell counting (trypan blue exclusion test) and indirectly by testing for the 3,(4,5-dimethylthiazol-2-yl)-2,5-diphenyl tetrazolium bromide (MTT)-positive cells. DNA fragmentation, as assessed by the content of nucleosome-bound DNA, was used as the apoptotic index (see Fig. 8).

For the concentration response of G/GO, the wild-type cells were treated with β-D-glucose (10 mM) and varied concentrations of GO (1, 5, and 10 milliunits/ml) for 12 h (Western blotting for Ku70 and Ku80) (see Fig. 3, *A* and *B*) and 24 h (cell viability and DNA fragmentation) (see Fig. 1). For the time response of G/GO, the wild-type cells were treated with β-D-glucose (10 mM) and GO (5 milliunits/ml) for 4, 12, and 24 h to measure the cell viability (see Fig. 2*A*), and Western blotting was used to determine the Ku70 and Ku80 levels in the whole cell extracts, the cytoplasmic extracts, and the nuclear extracts (see Fig. 3, *A* and *C*). As apoptotic indices, Western blotting for PARP cleavage, p53, Bcl-2, and Bax was performed in the whole cell extracts after the G/GO treatment for 4, 8, and 12 h (see Fig. 2*B*). To measure the amount of H_2O_2 generated by G/GO, the wild-type cells were treated with GO (1, 5, and 10 milliunits/ml) and with β-D-glucose (10 mM) for 12 and 24 h, respectively, and the culture medium was analyzed for H_2O_2. The H_2O_2 generated by the G/GO in the medium was determined using the method reported by Thurman *et al.* (43).

For one set of experiment, the wild-type cells were treated with or without G/GO (5 milliunits/ml) and cultured in the presence (caspase-3 inhibitor) or absence (control) of the caspase-3 inhibitor (5 μM; Z-Asp(Ome)-Glu(Ome)-Val-Asp(Ome)-CH_2F; Z-DEVD-fmk; Calbiochem, San Diego, CA) for 12 h. The Ku70 and Ku80 expression levels were determined by Western blotting (see Fig. 4*A*). Intracellular distribution of Ku70 or Ku80 was determined with immunofluorescence staining of Ku70 or Ku80 using fluorescein isothiocyanate-conjugated secondary antibody (see Fig. 5). To determine the cell viability (MTT-positive cells), the cells were treated with or without G/GO (3 and 5 milliunits/ml) and cultured in the presence of the caspase-3 inhibitor for 24 h (see Fig. 4*B*). All of the parameters were compared with those from the cells treated without G/GO. The caspase-3 inhibitor was dissolved in dimethyl sulfoxide. The final concentration of each vehicle was less than 0.1%. Each vehicle-treated cell was considered as the control. The drug concentration used in the study was adapted from a previous study (44).

To determine the effect of G/GO on Ku synthesis and degradation, the wild-type cells were pulsed or pulse-chased with [^{35}S]methionine with or without treatment of G/GO (5 milliunits/ml) and immunoprecipitated with anti-Ku70 or anti-Ku80 antibodies. The levels of Ku70 and Ku80 were determined in the whole cell extracts at 4 and 12 h or culture and in the cytoplasmic extracts and the nuclear extracts at 12 h of culture (see Figs. 9–12).

To determine the nuclear import of Ku proteins, an *in vitro* binding assay using GST or GST-importin α fusion protein was performed in the wild-type cells treated with or without G/GO (3 and 5 milliunits/ml) for 12 h. Bound protein levels were determined by Western blotting for Ku70, Ku80, and importin β. The importin β level was monitored in the wild-type cells treated with or without G/GO (3 and 5 milliunits/ml) for 12 h (see Fig. 13).

Preparation of Extracts—The wild-type cells were treated with or without G/GO (5 milliunits/ml) and cultured in the presence or absence of the caspase-3 inhibitor. In other experiments, the transfected cells (pcN-3, Ku D/N, $Ku70^+$, and $Ku80^+$ cells) were treated with or without G/GO (5 milliunits/ml) for 12 h. The cells were harvested with trypsin, washed with ice-cold phosphate-buffered saline (PBS) and lysed by adding a SDS solubilization buffer (125 mM Tris-HCl, pH 7.5, 5 mM EDTA, and 1% SDS). The lysates were then boiled for 5 min and centrifuged at 15,000 × *g* for 20 min. The supernatants were collected and used as the whole cell extracts. To prepare the cytoplasmic and nuclear extracts, the cells were harvested with trypsin, resuspended in 100 μl of the hypotonic buffer (10 mM Hepes, pH 7.9, 10 mM KCl, 1.5 mM $MgCl_2$, 0.5% Nonidet P-40, 0.5 mM dithiothreitol (DTT), and 0.5 mM phenylmethylsulfonyl fluoride), and placed on ice for 20 min. The extracts were centrifuged at 15,000 × *g* for 20 min at 4 °C. The supernatants were collected as the cytoplasmic extracts. The pellets were washed once with a hypotonic buffer, resuspended in 50 μl of the extraction buffer (20 mM Hepes, pH 7.9, 420 mM NaCl, 0.5 mM EDTA, 1.5 mM $MgCl_2$, 25% glycerol, 0.5 mM DTT, and 0.5 mM phenylmethylsulfonyl fluoride) and placed on ice for 20 min. The extracts were centrifuged at 15,000 × *g* for 20 min at 4 °C, and the supernatants were used as the nuclear extracts (45). The protein concentration was determined using the method reported by Bradford (46).

Western Blot Analysis—The whole cell extracts (50 μg of protein/lane), the cytoplasmic extracts (50 μg of protein/lane), and the nuclear extracts (25 μg of protein/lane) were loaded, separated by 8% SDS-polyacrylamide gel electrophoresis under reducing conditions, and transferred onto nitrocellulose membranes (Amersham Biosciences) by electroblotting. The transfer of the protein and the equality of the loading in the lanes was verified using reversible staining with Ponceau S. The membranes were blocked with 5% nonfat dry milk in TBS-T (Tris-buffered saline and 0.15% Tween 20) for 3 h at room temperature. The proteins were detected with polyclonal antibodies for Ku70 (1:1000; sc-1487), Ku80 (1:500; sc-1484), actin (1:1000; sc-1615), aldolase (1:500; sc-12059), and histone H1 (1;500; sc-8615) (all from Santa Cruz Biotechnology, Santa Cruz, CA) diluted in TBS-T containing 5% dry milk and incubated at 4 °C overnight. After washing in TBS-T, the immunoreactive proteins were visualized using goat anti-rabbit secondary antibodies conjugated to horseradish peroxidase, which was followed by enhanced chemiluminescence (Amersham Biosciences). To detect PARP cleavage, the rabbit polyclonal antibody for PARP (1:1000) (Santa Cruz Biotechnology, sc-7150) was used as the primary antibody. Western blotting for p53, Bcl-2, Bax, importin β, and actin were performed using mouse monoclonal antibody for p53 (1:200) (ParMingen/Beckton Dickinson Co., San Diego, CA; 554157), mouse monoclonal antibody for Bcl-2 (1:500) (Transduction Laboratories, San Diego, CA; 610538), mouse monoclonal antibody for Bax (1:500) (Transduction Laboratories, San Diego, CA; 610983), mouse monoclonal antibody for importin β (1:2000) (Alexis Biochemicals, San Diego, CA; NTF97), and polyclonal antibody for actin (1:1000) (Santa Cruz Biotechnology; sc-1615) as the primary antibodies, respectively. Actin was used for the protein loading control, whereas aldolase A and histone H1 were used for the cytoplasmic and nuclear controls, respectively. Exactly equal amounts of protein, determined by Bradford method (46), were loaded in each lane. The Western result presented in each figure is the representative of five separate experiments.

Electrophoretic Mobility Shift Assay—Electrophoretic mobility shift assay was carried out by a slight modification of the method reported by Li *et al.* (47). The nuclear extracts (2 μg of nuclear protein) of wild-type, pcN-3, and KuD/N cells were incubated with the ^{32}P-labeled double-stranded oligonucleotide, 5′-GGGCCAAGAATCTTAGCAGTTTCGGG-3′, in a buffer containing 12% glycerol, 12 mM Hepes, pH 7.9, 1 mM EDTA, 1 mM DTT, 25 mM KCl, 5 mM $MgCl_2$, and 0.04 μg/ml poly(dI-dC) at room temperature for 30 min. The reaction mixtures were subjected to electrophoretic separation at room temperature on a nondenaturing 5% acrylamide gel at 30 mA using 0.5× Tris-borate-EDTA buffer. The gels were dried at 80 °C for 1 h and exposed to the radiography film for 6–18 h at −70 °C with intensifying screens.

Cell Counting and MTT Assay—Cell viability was determined directly by counting with hemocytometer by a trypan blue exclusion test (0.2% trypan blue) and indirectly by a colorimetric immunoassay (MTT assay). For the trypan blue exclusion test, the cells were plated at 2×10^4 cells/well in a 24-well culture plate and then incubated for 24 h. The number of cells was counted with a hemocytometer using 0.2% trypan blue. For the MTT assay, the cells (1.5×10^4 cells/well) were plated onto a 96-well culture plate and cultured for 24 h. MTT (2.5 mg/ml) was added, and the reaction mixture was incubated at 37 °C for 4 h. Cellular formazan was extracted with acidic propan-2-ol, and the absorbance was measured using a dual wavelength automatic plate reader at 570 nm/630 nm (48). Viable cells were expressed as the MTT-positive cells. The MTT-positive cells shown in the wild-type cells or the pcN-3 cells treated without G/GO (*Wild* for Figs. 1*B* and 4*B* and *pcN-3* for Fig. 8*B*) was considered to be 100%. The relative MTT-positive cells are expressed as a percentage of the value.

Quantitation of DNA Fragmentation—The nucleosomes were quantified using a sandwich enzyme-linked immunosorbent assay (Cell Death Detection ELISA^{plus} kit; Roche Molecular Biochemicals GmbH, Germany). In brief, the wild-type cells (5×10^4 cells/well) were treated with various GO concentrations (1, 3, 5, and 10 milliunits) with 10 mM glucose for 24 h (see Fig. 1*C*). The transfected cells (pcN-3, KuD/N, $Ku70^+$, and $Ku80^+$ cells) were treated with 3 milliunits of GO using 10 mM glucose and cultured for 24 h (see Fig. 8*C*). The cells were detached, and 1×10^5 cells were lysed. After cell lysis, the nucleosome-bound

DNA was quantified using biotin-coupled mouse monoclonal anti-histone antibody as the capturing antibody, peroxidase-conjugated mouse monoclonal anti-DNA antibody as the detecting antibody, and 2,2′-azio-di[3-ethylbenhioazolin-sulfonate as a developing reagent. The relative increase in the number of nucleosomes in the cell lysate, determined at 405 nm, was expressed as an enrichment factor. The enrichment factor of the wild-type cells or the pcN-3 cells treated without G/GO was considered to be 1 (*Wild* for Fig. 1*C* and *pcN-3* for Fig. 8*C*).

Immunofluorescence Staining—The wild-type cells (5×10^4 cells/well) were grown on Lab-Tek chamber slides (Nunc Inc., Naperville, IL) overnight and treated with or without G/GO (5 milliunits/ml) in the presence (caspase-3 inhibitor) or absence (control) of the caspase-3 inhibitor (5 μM; Z-Asp(Ome)-Glu(Ome)-Val-Asp(Ome)-CH_2F; Z-DEVD-fmk, Calbiochem) for 12 h. The cells were washed with PBS, air-dried, and fixed in cold 100% methanol for 10 min at room temperature (49). The fixed cells were first blocked for 30 min in a blocking solution (5% goat serum, 1% bovine serum albumin, and 0.1% gelatin in PBS containing 0.001% sodium azide) and then incubated for 60 min at room temperature with polyclonal antibody for Ku70 (1:200) (Santa Cruz Biotechnology; sc-1487) or Ku80 (1:200) (Santa Cruz Biotechnology; sc-1484) diluted in blocking solution. After washing with PBS, antibody binding was detected by the application of fluorescein isothiocyanate (Cappel Laboratories, Durham, NC)-conjugated secondary antibody (anti-goat IgG antibody) dilated at a 1:100 dilution with blocking solution for 60 min. The cells were covered with the antifade medium Vectashield (Vector Laboratories, Burlingame, CA) containing 4′,6′-diamidino-2-phenylindole (DAPI) (0.25 μg/ml end concentration) following two more washes in PBS and a postfixation step with 3.7% paraformaldehyde for 5 min. The preparations were stored for at least 1 h to allow saturation with DAPI to specifically stain the nucleus. Immunofluorescence images for Ku proteins and the images of the nucleus stained with DAPI were obtained using a Zeiss LSM510 confocal microscope (see Fig. 5).

[^{35}S]Methionine Experiment—For the pulse experiment, the wild-type cells (5×10^6 cells/well) were treated with or without G/GO (5 milliunits/ml) and pulsed with [^{35}S]methionine (final concentration, 100 μCi/ml) (Amersham Biosciences) during the last 4 h of each incubation. Briefly, the cells were treated with or without G/GO for either 4 or 12 h. [^{35}S]Methionine was added to the cells at the start of the incubation (4 h of treatment) or after 8 h of culturing with G/GO (12 h of treatment). Thus, the pulsed cells were cultured for 4 h. During pulsing with [^{35}S]methionine, the cells were cultured in methionine- and cysteine-free DMEM containing the dialyzed 10% fetal bovine serum. For the pulse-chase experiment, the wild-type cells (5×10^6 cells/well) were preincubated in methionine- and cysteine-free DMEM containing the dialyzed 10% fetal bovine serum and [^{35}S]methionine (final concentration, 100 μCi/ml) for 4 h. The cells were then washed with complete DMEM and cultured for 4 and 12 h with or without the G/GO treatment (5 milliunits/ml). At each time point, the cells were lysed in a radioimmunoprecipitation buffer (10 mM Tris, pH 7.4, 1.0% Nonidet P-40, 0.15 M NaCl, 1 mM EDTA, 1 mM EGTA, 0.5% sodium deoxycholate, and 0.5 mM phenylmethylsulfonyl fluoride) (50, 51). The cytoplasmic extracts and the nuclear extracts from the cells were prepared as described above. Either the whole cell extracts (100 μg of protein), the cytoplasmic extracts (100 μg of protein), or the nuclear extracts (50 μg of protein) were immunoprecipitated with the anti-Ku70 or anti-Ku80 antibodies (final concentration, 5 μg/ml), collected by protein G-agarose beads (Sigma) at 4 °C, resolved by SDS-PAGE, and then visualized by autoradiography. The density shown in the cells treated without G/GO at 0 h (see Figs. 9 and 11) or at 12 h (see Figs. 10 and 12) was considered to be 100%. The relative densities were expressed as a percentage of that value at either 0 h (see Figs. 9 and 11) or 12 h (see Figs. 10 and 12).

In Vitro Binding Assay—Bacteria transformed with plasmids encoding GST and GST-importin-α fusion protein were cultured overnight at 37 °C, then isopropyl β-D-thiogalactopyranoside (0.5 mM) was added, and incubation was continued for another 3 h to induce protein expression. The bacteria were collected by centrifugation and were resuspended in STE buffer (10 mM Tris, pH 8.0, 150 mM NaCl, and protease inhibitors). The bacteria were lysed by incubation with 0.1 mg/ml lysozyme at 4 °C for 15 min, followed by the addition of 5 mM DTT and 1.5% *N*-laurylsarcosyl (sarkosyl) to recover GST and GST-importin-α. The bacteria were disrupted by brief sonication on ice, and the lysates were clarified by centrifugation at 10,000 $\times$ *g* for 15 min. Each supernatant was incubated at 4 °C for 1 h with 200 μl of glutathione-agarose bead (Sigma). The agarose bead was collected and washed four times with STE buffer. GST and GST-importin-α fusion protein were eluted from the glutathione-agarose bead as described (52), and free glutathione was removed using Sephadex G-50 column. The wild-type cells treated with or without G/GO (3, 5 milliunits/ml) for 12 h were lysed in the lysis buffer containing 50 mM Tris, pH 7.4, 100 mM NaCl, 2 mM $MgCl_2$, 1 mM DTT, 1% Nonidet P-40, 10% glycerol, and protease inhibitors. The cleared lysates (200 μg) were incubated overnight with 10 μg of GST or GST-importin-α bound to glutathione-agarose beads at 4 °C. The agarose beads were collected and washed four times with lysis buffer. The bound proteins were released by boiling for 5 min with 50 μl of SDS sample buffer and detected by SDS-PAGE and Western blot analysis using anti-Ku70, anti-Ku80, and anti-importin β antibodies (see Fig. 13*A*).

Statistical Analysis—The results are expressed as the means ± S.E. of five separate experiments. The analysis of the variance followed by the Newman-Keul's test was used for statistical analysis (53). $p < 0.05$ was considered statistically significant.

RESULTS

Concentration and Time Responses of G/GO for H_2O_2 Production and the Apoptotic Indices (Cell Viability, DNA Fragmentation, PARP Cleavage, and Expression Changes of p53, Bcl-2, and Bax) in AR42J Cells—Because the susceptibility of the cells to G/GO-mediated damage varies among the different cell types, the cell strains, and passage numbers within the same strain (54–56), the concentration and time responses of G/GO to the wild-type AR42J cells were determined. The H_2O_2 content in the medium released from the cells were 0.85 ± 0.04 nmol/ml at 12 h and 7.31 ± 1.59 nmol/ml at 24 h, respectively. The cells treated with β-D-glucose (10 mM) and various GO (1, 5, and 10 milliunits/ml) concentrations released H_2O_2 into the medium in amounts of 2.84 ± 1.12, 17.11 ± 2.09, and 32.08 ± 1.61 nmol/ml at 12 h and 30.17 ± 5.02, 64.03 ± 8.10, and 115.16 ± 7.31 nmol/ml at 24 h. To determine the relationship between the oxidative stress and apoptosis, the concentration response of G/GO (1, 5, and 10 milliunits/ml) for the cell viability and the nucleosome-bound DNA was determined in the cells after the 24-h treatment with G/GO. At 24 h, the number of viable cells, determined by trypan blue exclusion test (Fig. 1*A*) and MTT assay (Fig. 1*B*), was significantly lower at GO 5 and 10 milliunits/ml, which was in parallel with the increases in the nucleosome-bound DNA, an index of DNA fragmentation (Fig. 1*C*). For the time response of G/GO, the cells treated with G/GO (5 milliunits/ml) were cultured for 4, 12, and 24 h, and the viable cells were counted with a trypan blue exclusion test. At a GO concentration of 5 milliunits/ml, the number of viable cells was lower at 12 and 24 h (Fig. 2*A*). The number of viable cells ($\times 10^4$ cells/ml) from the cells treated with G/GO were 7.70 ± 0.23, 7.31 ± 0.28, 4.11 ± 0.29, and 2.41 ± 0.21 at the start of the experiment and at 4, 12, and 24 h of culture, respectively (Fig. 2*A*). Western blotting analysis for p53, Bax, and Bcl-2 showed a significant induction of p53 and Bax accompanied with a loss of Bcl-2 in the wild-type cells treated with G/GO (5 milliunits/ml) for 12 h. PARP cleavage to the 85-kDa peptides was detected at 8 and 12 h.

Concentration and Time Responses of G/GO for Ku Expression in AR42J Cells—To monitor the changes in Ku70 and Ku80 during G/GO-induced apoptosis, the concentration and time responses of G/GO for Ku expression were determined at 12 h. Both Ku70 and Ku80 levels in the whole cell extracts were unaltered by the G/GO treatment (Fig. 3*A*). Even high G/GO (10 milliunits/ml) concentration for 24 h did not affect the total levels of both Ku70 and Ku80. However, the nuclear Ku70 and Ku80 levels were drastically lowered with increasing GO concentrations and culture time (Fig. 3, *B* and *C*). The decreases in the nuclear Ku70 and Ku80 were evident at GO 5 milliunits/ml for a 12-h culture. The nuclear Ku70 level was almost lost at GO 5 milliunits/ml for 12 h (Fig. 3*B*), whereas the nuclear Ku80 almost disappeared at GO 5 milliunits/ml for 12 h (Fig. 3*C*). The loss of nuclear Ku70 and Ku80 were more evident at GO 10 milliunits/ml for a 24-h culture. Interestingly, cytoplasmic

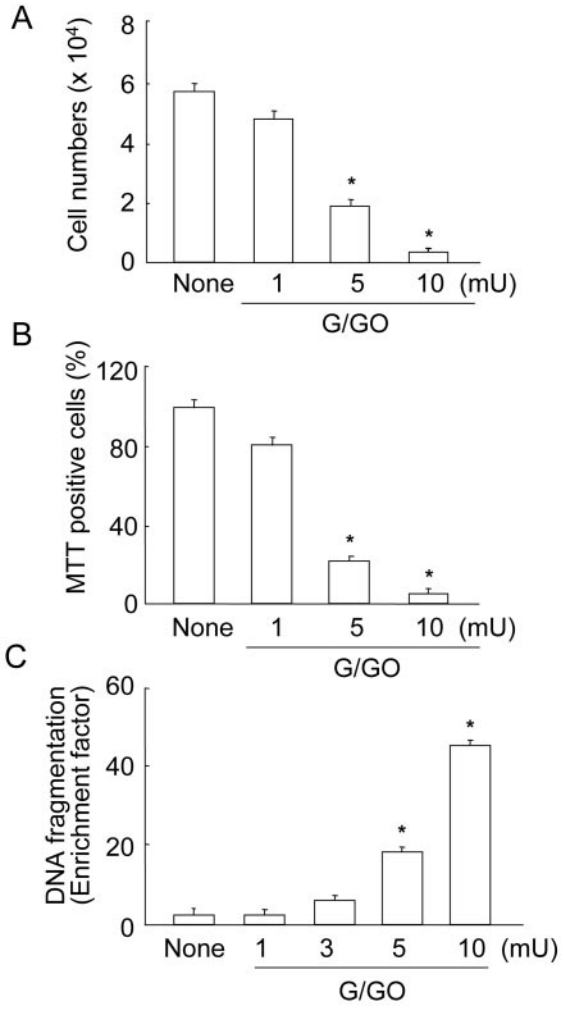

FIG. 1. **Concentration response of G/GO for cell viability and DNA fragmentation in AR42J cells.** The wild-type cells were treated with β-D-glucose (10 mM) and varying GO concentrations (1, 5, and 10 milliunits/ml) for 24 h. The cell viability was determined directly by trypan blue exclusion test (*A*) and indirectly by MTT assay (*B*). The MTT-positive cells shown in the cells treated without G/GO (*None*) were considered to be 100%. The relative MTT-positive cells were expressed as percentages of that value. Enzyme-linked immunosorbent assay was used to assess the extent of DNA fragmentation as the content of nucleosome-bound DNA (*C*). The relative increase in the number of nucleosomes in the cell lysate, determined at 405 nm, was expressed as an enrichment factor. The enrichment factor of the cells treated without G/GO (*None*) was considered to be 1. Each *bar* represents the mean ± S.E. of five separate experiments. *, $p < 0.05$ *versus* the cells treated without G/GO (*None*). *G/GO*, the cells treated with G/GO; *bar 1*, 1 milliunit/ml; *bar 3*, 3 milliunits/ml; *bar 5*, 5 milliunits/ml; *bar 10*, 10 milliunits/ml.

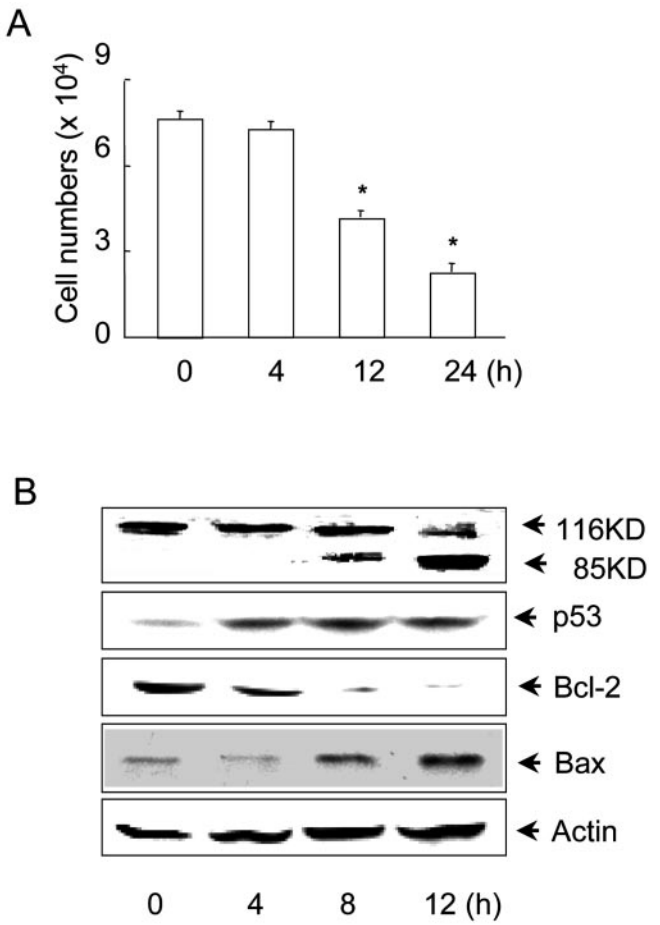

FIG. 2. **Time responses of G/GO for cell viability, PARP cleavage, and expression changes of p53, Bcl-2, and Bax in AR42J cells.** For the time response of G/GO, the wild-type cells were treated with β-D-glucose (10 mM) and GO (5 milliunits/ml) for 12 h (PARP cleavage, p53, Bcl-2, and Bax) or 24 h (cell viability). The viable cell numbers were determined by trypan blue exclusion test (*A*). Each *bar* represents the mean ± S.E. of five separate experiments. *, $p < 0.05$ *versus* 0 h. Western blotting for PARP and its cleavage product as well as p53, Bcl-2, and Bax were used as the apoptotic indices (*B*). Actin was used for the protein loading control. The Western result in each lane is the representative of five separate experiments.

Ku80 tended to be increased by G/GO in a concentration- and time-dependent manner, whereas cytoplasmic Ku70 was slightly affected by the G/GO treatment.

Effect of Caspase-3 Inhibitor on Ku Expression, Cell Viability, and Intracellular Distribution of Ku in AR42J Cells Treated with or without G/GO—The wild-type cells were treated with G/GO (GO 5 milliunits/ml) in the presence or absence (control) of the caspase-3 inhibitor for 12 h. Western blot results showed that G/GO induced significant decreases in the nuclear Ku70 and Ku80 levels, which was prevented by treatment with the caspase-3 inhibitor (Fig. 4*A*). The cytoplasmic Ku70 levels were slightly altered by G/GO, whereas the cytoplasmic Ku80 levels were increased by G/GO. Treatment with caspase-3 inhibit7or had no effect on these changes in the cytoplasmic Ku70 and Ku80. G/GO induced cell death in a concentration-dependent manner, as determined by the number of the MTT-positive cells (Fig. 4*B*). The number of MTT-positive cells shown in the wild-type cells treated with G/GO (None) was considered to be 100%. The relative number of MTT-positive cells in the cells treated with G/GO at 3 and 5 milliunits/ml were 58.79 ± 2.97 and 28.75 ± 3.03, respectively, in the absence of the caspase-3 inhibitor, whereas those cultured in the presence of the caspase-3 inhibitor were 90.06 ± 4.39 and 74.90 ± 8.09, respectively. Caspase-3 inhibitor prevented G/GO-induced cell death, suggesting the involvement of capase-3 activation in oxidative stress-induced apoptosis.

Intracellular distribution of Ku70 and Ku80 of the wild-type cells was determined by immunofluorescence staining of Ku proteins using fluorescein isothiocyanate-conjugated secondary antibody. Because pancreatic acinar cells were grown as acinus formation as reported previously (57, 58), one representative acinus was visualized. Immunofluorescence staining revealed that Ku70 and Ku80 were abundant both in the cytoplasm and the nucleus in the wild-type cells treated without G/GO in the absence of the caspase-3 inhibitor (Fig. 5*A*). Treatment of the caspase-3 inhibitor has no effect on intracellular distribution of Ku70 and Ku80 in the wild-type cells treated without G/GO (Fig. 5*B*). However, G/GO treatment in the absence of the

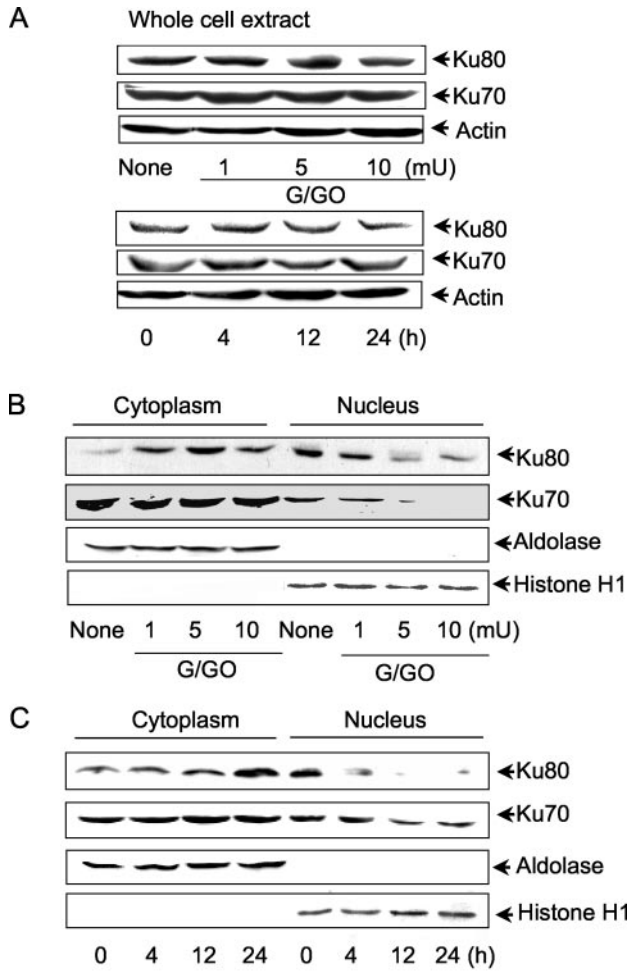

FIG. 3. **Concentration and time responses of G/GO for Ku expression in AR42J cells.** For the concentration response of G/GO, the wild-type cells were treated with β-D-glucose (10 mM) and varying GO concentrations (1, 5, and 10 milliunits/ml) for 12 h. For the time response of G/GO, the wild-type cells were treated with β-D-glucose (10 mM) and GO (5 milliunits/ml) for 4, 12, and 24 h. Ku expression was determined by Western blotting for Ku70 and Ku80 in the whole cell extracts (*A*), the cytoplasmic extracts, and the nuclear extracts (*B* and *C*). Actin was used for the protein loading control (*A*). Aldolase and histone H1 were used as the cytoplasmic and nuclear controls, respectively (*B* and *C*). Exactly equal amounts of protein were loaded in each lane. The Western result in each lane is the representative of five separate experiments. *None*, cells treated without G/GO; *G/GO*, cells treated with G/GO; *lane 1*, 1 milliunit/ml; *lane 5*, 5 milliunits/ml; *lane 10*, 10 milliunits/ml.

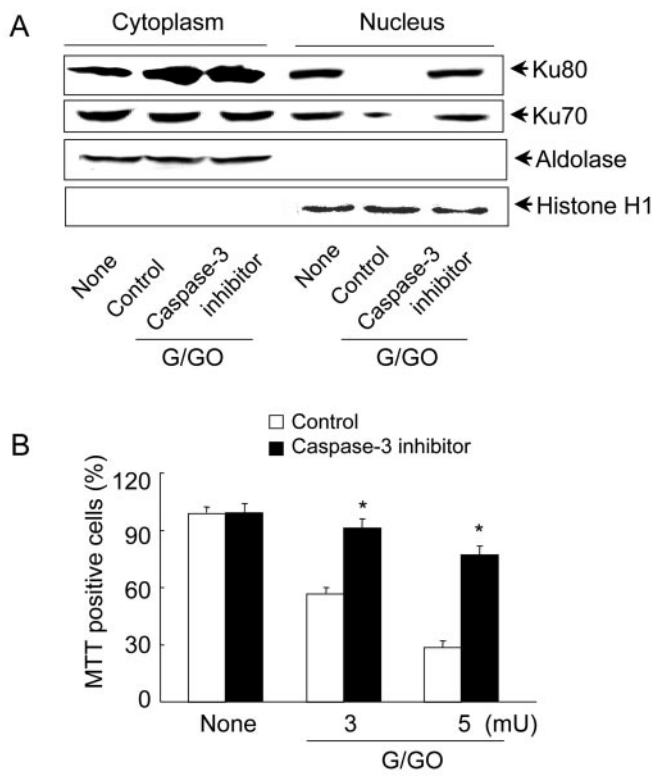

FIG. 4. **Effect of caspase-3 inhibitor on Ku expression and cell viability of AR42J cells treated with or without G/GO.** The wild-type cells were treated with G/GO (5 milliunits/ml) in the presence or absence of the caspase-3 inhibitor (5 μM; Z-DEVD-fmk) for 12 h. Western blot analysis was performed to analyze Ku70 and Ku80 in the cytoplasmic and nuclear extracts (*A*). Aldolase and histone H1 were used as the cytoplasmic and nuclear controls, respectively. Exactly equal amount of protein was loaded in each lane. The Western result in each lane is the representative of five separate experiments. The cell viability was determined by the number of the MTT-positive cells (*B*). The number of the MTT-positive cells shown in the cells treated without G/GO (*None*) was considered to be 100%. The relative MTT-positive cells were expressed as percentages of this value. Each *bar* represents the mean ± S.E. of five separate experiments. *, $p < 0.05$ *versus* the corresponding control. *Control*, cells treated with a vehicle (dimethyl sulfoxide); *Caspase-3 inhibitor*, cells treated with caspase-3 inhibitor; *None*, cells treated without G/GO; *G/GO*, cells treated with G/GO; *bar 3*, 3 milliunits/ml; *bar 5*, 5 milliunits/ml).

caspase-3 inhibitor resulted in the nuclear loss of both Ku70 and Ku80, shown as undetectable fluorescence staining in the nucleus, determined by DAPI counterstaining of the nucleus (Fig. 5*A*). AR42J cells have relatively large nuclei as previous immunofluorescence staining reported (57). The caspase-3 inhibitor prevented G/GO-induced nuclear loss of Ku70 and Ku80 in the wild-type cells (Fig. 5*B*). This is in agreement with Western results of Ku70 and Ku80 expression levels shown in Fig. 4*A*.

Effect of G/GO on Expression or DNA Binding Activity of Ku in AR42J Cells and the Transfected Cells (pcN-3, KuD/N, Ku70$^+$, and Ku80$^+$ Cells)—In the wild-type and pcN-3 cells, 12 h of treatment with G/GO induced slight changes in the cytoplasmic Ku70 and Ku80 levels and significant decreases in the nuclear Ku70 and Ku80 levels, respectively (Fig. 6). In the Ku70$^+$ cells and Ku80$^+$ cells, the cytoplasmic Ku70 and Ku80 levels were higher in both cells treated with and without G/GO compared with those in the wild-type and pcN-3 cells. The G/GO-induced decrease in the nuclear Ku70 and Ku80 levels were prevented in both Ku70$^+$ and Ku80$^+$ cells. However, the prevention against the G/GO-induced loss of nuclear Ku70 and Ku80 were more evident in the Ku80$^+$ cells. This result demonstrates that both Ku70 and Ku80 contribute to the stability of the other Ku subunits. G/GO resulted in a loss of the Ku-DNA binding activity in the wild-type and pcN-3 cells. The loss of the Ku-DNA binding activity was observed in the Ku D/N cells even without G/GO (Fig. 7).

Effect of G/GO on Cell Viability and DNA Fragmentation in AR42J Cells and the Transfected Cells (pcN-3, KuD/N, Ku70$^+$, and Ku80$^+$ Cells)—In the wild-type and pcN-3 cells, 24 h of treatment with G/GO (3 and 5 milliunits/ml) decreased the number of viable cells, as determined directly by the trypan blue dye exclusion test (Fig. 8*A*) and indirectly by MTT assay (Fig. 8*B*), as well as the extent of DNA fragmentation determined by the nucleosome-bound DNA (Fig. 8*C*). The decrease in cell viability (the viable cell number and MTT-positive cells) and the increase in DNA fragmentation induced by G/GO treatment were inhibited in the Ku70$^+$ and Ku80$^+$ cells. The G/GO-induced cell death and apoptotic DNA fragmentation was accelerated in the KuD/N cells. The relative increase in the number of nucleosomes in the cell lysate was expressed as an

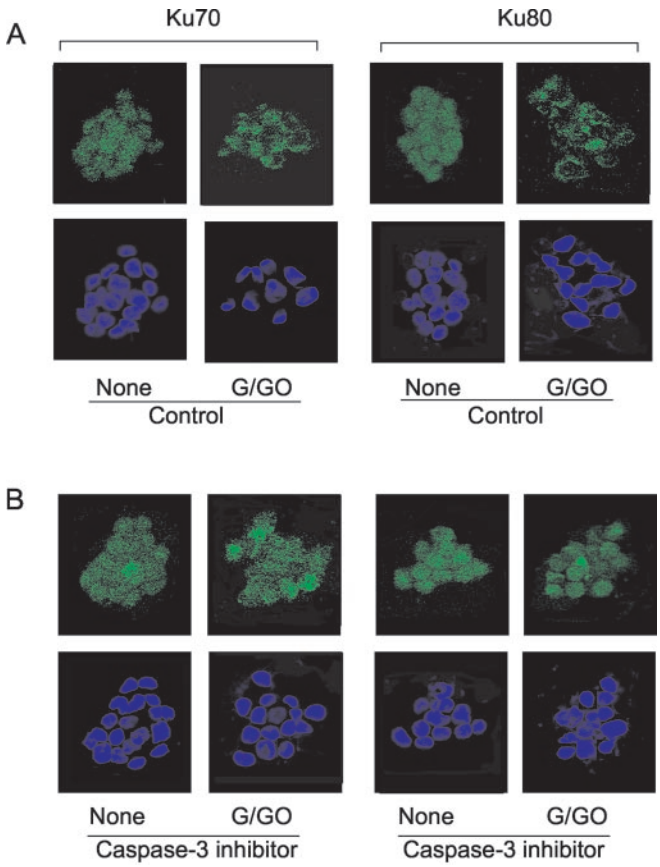

FIG. 5. **Intracellular distribution of Ku70 and Ku80 in AR42J cells treated with or without G/GO in the presence or absence of the caspase-3 inhibitor.** The wild-type cells were treated with or without G/GO (5 milliunits/ml) in the presence or absence of the caspase-3 inhibitor (5 μM, Z-DEVD-fmk) for 12 h. The cells were immunostained with polyclonal antibody for Ku70 (*left panels*) and Ku80 (*right panels*). The immunoreactive proteins were visualized using fluorescein isothiocyanate-conjugated anti-goat IgG antibody (*green*, *upper panels*) with DAPI counterstaining (*blue*, *lower panels*) of the same field containing one acinus. Intracellular distribution of Ku70 and Ku80 and the nucleus of the cells were observed by Zeiss LSM510 confocal microscope. Loss of Ku proteins in the nucleus of the cells treated with G/GO in the absence of the caspase-3 inhibitor (*Control*, *G/GO*), showing undetectable fluorescence staining, determined by DAPI counterstaining of the nucleus. The result is the representative of five separate experiments. *Control*, cells cultured in the absence of the caspase-3 inhibitor (*A*); *Caspase-3 inhibitor*, cells cultured in the presence of the caspase-3 inhibitor (*B*); *None*, cells treated without G/GO; *G/GO*, cells treated with G/GO.

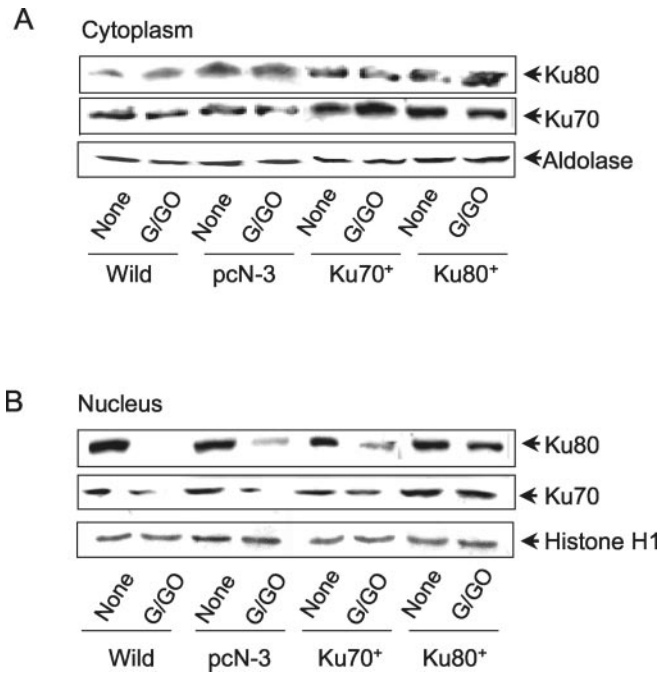

FIG. 6. **Effect of G/GO on Ku expression in AR42J cells and the transfected cells (pcN-3, Ku70$^+$, and Ku80$^+$ cells).** The wild-type, pcN-3, Ku70$^+$, and Ku80$^+$ cells were treated with or without G/GO (5 milliunits/ml) for 12 h. Ku expression was determined by Western blotting for Ku70 and Ku80 in the cytoplasmic (*A*) and nuclear extracts (*B*). Aldolase and histone H1 were used as the cytoplasmic and nuclear controls, respectively. Exactly equal amounts of protein were loaded in each lane. The Western result in each lane is the representative of five separate experiments. *Wild*, nontransfected cells; *pcN-3*, cells transfected with the control pcDNA3 vector; *Ku70*$^+$, cells transfected with the Ku70 expression gene; *Ku80*$^+$, cells transfected with the Ku80 expression gene; *None*, cells treated without G/GO; *G/GO*, cells treated with G/GO.

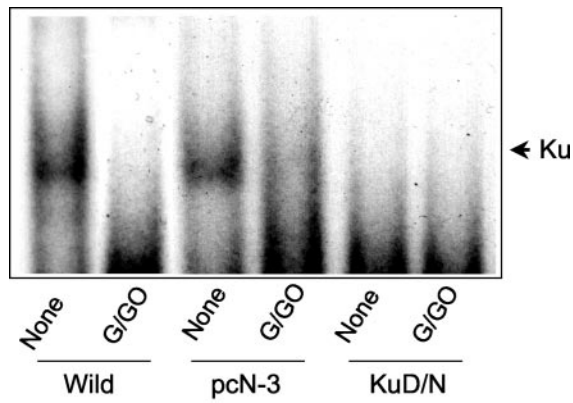

FIG. 7. **Ku-DNA binding activity in the nuclear extract of AR42J cells and the transfected cells (pcN-3 and KuD/N cells).** The wild-type, pcN-3, and KuD/N cells were treated with or without G/GO (5 milliunits/ml) for 12 h. The Ku-DNA binding activity was determined using 2 μg of the nuclear protein by electrophoretic mobility shift assay. The result is the representative of five separate experiments. *Wild*, nontransfected cells; *pcN-3*, cells transfected with the control pcDNA3 vector; *KuD/N*, cells transfected with the Ku dominant negative mutant; *None*, cells treated without G/GO; *G/GO*, cells treated with G/GO.

enrichment factor for DNA fragmentation. Without the G/GO treatment, the extent of DNA fragmentation was not changed in the wild-type cells (1.00 ± 0.08) and the transfected cells (1.00 ± 0.06). The amount of DNA fragmentation was changed to 4.71 ± 0.02, 5.22 ± 0.18, 2.90 ± 0.09, 2.91 ± 0.26, and 6.52 ± 0.08 in the wild-type, the pcN-3, the Ku70$^+$, the Ku80$^+$, and the KuD/N cells after treatment with G/GO (3 milliunits/ml), respectively (Fig. 8*C*). This result suggests that Ku70 and Ku80 overexpression prevent cell death and that the loss of the Ku proteins induces apoptotic cell death.

Effect of G/GO on Synthesis and Degradation of Ku in AR42J Cells—To determine the mechanism of the G/GO-induced changes in Ku expression in the whole cell extracts, the cytoplasmic extracts, and the nuclear extracts, the wild-type cells were pulsed or pulse-chased with [^{35}S]methionine with or without the G/GO treatment for either 4 or 12 h. For the pulse experiment, the cells were treated with or without G/GO and pulsed with [^{35}S]methionine during the last 4 h of each incubation (Figs. 9 and 10). The syntheses of both Ku70 and Ku80, as determined by the [^{35}S]methionine pulse, were significantly increased by G/GO in the whole cell extracts when compared with the cells without the G/GO treatment at 4 and 12 h of incubation. The density of [^{35}S]methionine-Ku80 or [^{35}S]methionine-Ku70 shown in the cells treated without G/GO at 0 h was considered to be 100%. The relative densities of [^{35}S]methionine-Ku80 in the cells treated without G/GO were 109.5 ±

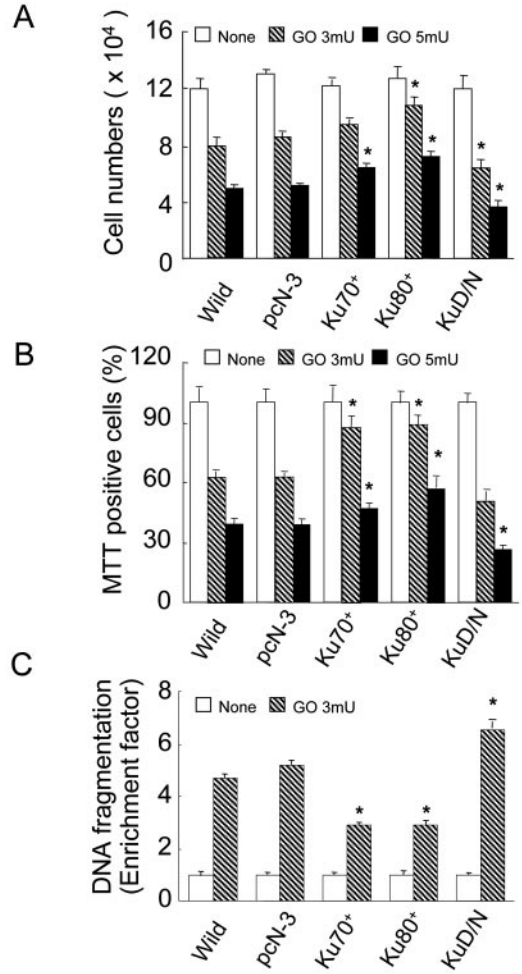

FIG. 8. **Effect of G/GO on cell viability and DNA fragmentation in AR42J cells and the transfected cells (pcN-3, KuD/N, Ku70$^+$, and Ku80$^+$ cells).** The wild-type cells and the transfected cells (pcN-3, KuD/N, Ku70$^+$, and Ku80$^+$ cells) were treated with or without G/GO (3 and 5 milliunits/ml) for 24 h. Cell viability was determined directly by trypan blue exclusion test (*A*) and indirectly by MTT assay (*B*). The MTT-positive cells shown in pcN-3 cells were considered to be 100%. The relative MTT-positive cells were expressed as percentages of the pcN-3 cells. Enzyme-linked immunosorbent assay was used to assess the extent of DNA fragmentation as the content of nucleosome-bound DNA (*C*). The relative increase in nucleosomes in the cell lysate, as determined at 405 nm, was expressed as an enrichment factor. The enrichment factor of the wild-type cells treated without G/GO (*Wild*, *None*) was considered to be 1. Each *bar* represents the mean ± S.E. of five separate experiments. *, $p < 0.05$ *versus* the corresponding pcN-3. *Wild*, nontransfected cells; *pcN-3*, cells transfected with the control pcDNA3 vector; *Ku70$^+$*, cells transfected with the Ku70 expression gene; *Ku80$^+$*, cells transfected with the Ku80 expression gene; *KuD/N*, cells transfected with the Ku dominant negative mutant; *None*, cells treated without G/GO. *GO 3mU*, cells treated with 3 milliunits G/GO/ml); *GO 5mU*, cells treated with 5 milliunits of G/GO/ml).

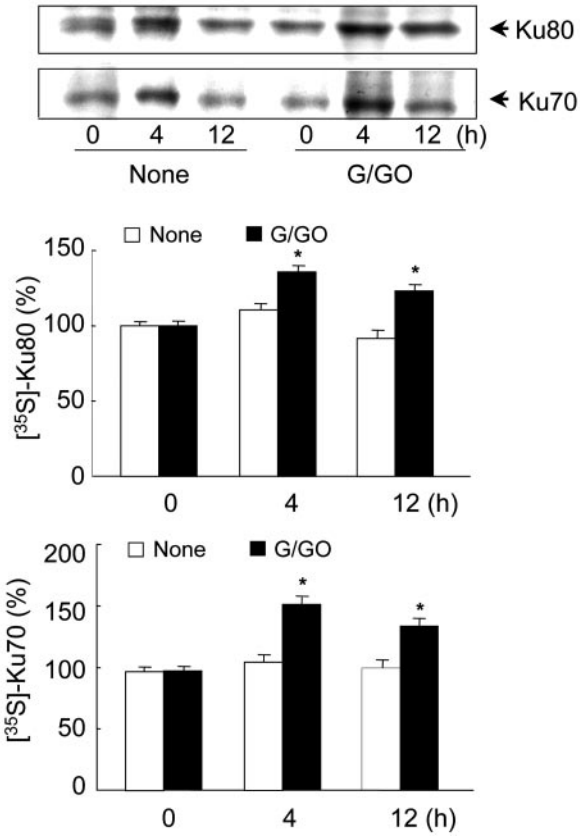

FIG. 9. **Effect of G/GO on Ku synthesis in AR42J cells.** For the pulse experiment, the wild-type cells were treated with or without G/GO and pulsed with [^{35}S]methionine during the last 4 h of each incubation. The density shown in the cells treated without G/GO (*None*) at 0 h was considered to be 100%. The relative densities are expressed as percentages of this value at 0 h. Each *bar* represents the mean ± S.E. of five separate experiments. *, $p < 0.05$ *versus* corresponding to the untreated value at each time point (4 or 12 h). *None*, cells treated without G/GO; *G/GO*, the cells treated with G/GO (5 milliunits/ml); *[^{35}S]-Ku80*, [^{35}S]methionine-Ku80; *[^{35}S]-Ku70*, [^{35}S]methionine-Ku70.

2.11 and 86.82 ± 1.51, and those treated with G/GO were 129.81 ± 2.01 and 114.70 ± 1.21 at 4 and 12 h of culture, respectively. The relative densities of [^{35}S]methionine-Ku70 in the cells treated without G/GO were 104.4 ± 2.51 and 99.56 ± 2.00, and those treated with G/GO were 143.51 ± 2.61 and 133.60 ± 2.21 at 4 and 12 h of culture, respectively (Fig. 9). However, the G/GO-induced increase in Ku70 and Ku80 synthesis was only shown in the cytoplasmic extracts and not in the nuclear extracts at 12 h of culture (Fig. 10). When the densities of [^{35}S]methionine-Ku80 and [^{35}S]methionine-Ku70 in the cells treated without G/GO were considered to be 100%, [^{35}S]methionine-Ku80 in the cells treated with G/GO were 147.98 ± 2.90 in the cytoplasmic extracts and 96.31 ± 1.01 in the nuclear extracts. The relative densities of [^{35}S]methionine-Ku70 in the cells treated with G/GO were 148.84 ± 2.89 in the cytoplasmic extracts and 89.68 ± 1.00 in the nuclear extracts. For the pulse-chase experiment, the cells were preincubated with [^{35}S]methionine for 4 h and then cultured for 4 and 12 h with or without the G/GO treatment. At each time point, the amount of Ku expression was determined in the whole cell extracts (Fig. 11), the cytoplasmic extracts, and the nuclear extracts (Fig. 12). The Ku70 and Ku80 expression levels were decreased by G/GO in the whole cell extracts when compared with the cells without G/GO treatment at 4 and 12 h of culture. The relative densities of [^{35}S]methionine-Ku80 in the cells treated without G/GO were 95.22 ± 2.01 and 83.32 ± 2.01, and those treated with G/GO were 71.42 ± 2.10 and 53.02 ± 1.15 at 4 and 12 h, respectively. The relative densities of [^{35}S]methionine-Ku70 in the cells treated without G/GO were 93.31 ± 2.21 and 84.42 ± 2.03, and those treated with G/GO were 75.51 ± 2.31 and 66.60 ± 2.01 at 4 and 12 h, respectively. At 12 h of culture, G/GO decreased the Ku70 and Ku80 expression levels both in the cytoplasmic extracts and the nuclear extracts (Fig. 12). When the densities of [^{35}S]methionine-Ku80 and [^{35}S]methionine-Ku70 in the cells treated without G/GO were considered to be 100%, the amounts of [^{35}S]methionine-Ku80 in the cells treated with G/GO were 78.22 ± 1.99 in the cytoplasmic extracts and 59.70 ± 1.21 in the nuclear extracts at 12 h of culture. The relative densities of [^{35}S]methionine-Ku70 in the cells treated with G/GO were 79.32 ± 1.89 in the cytoplasmic

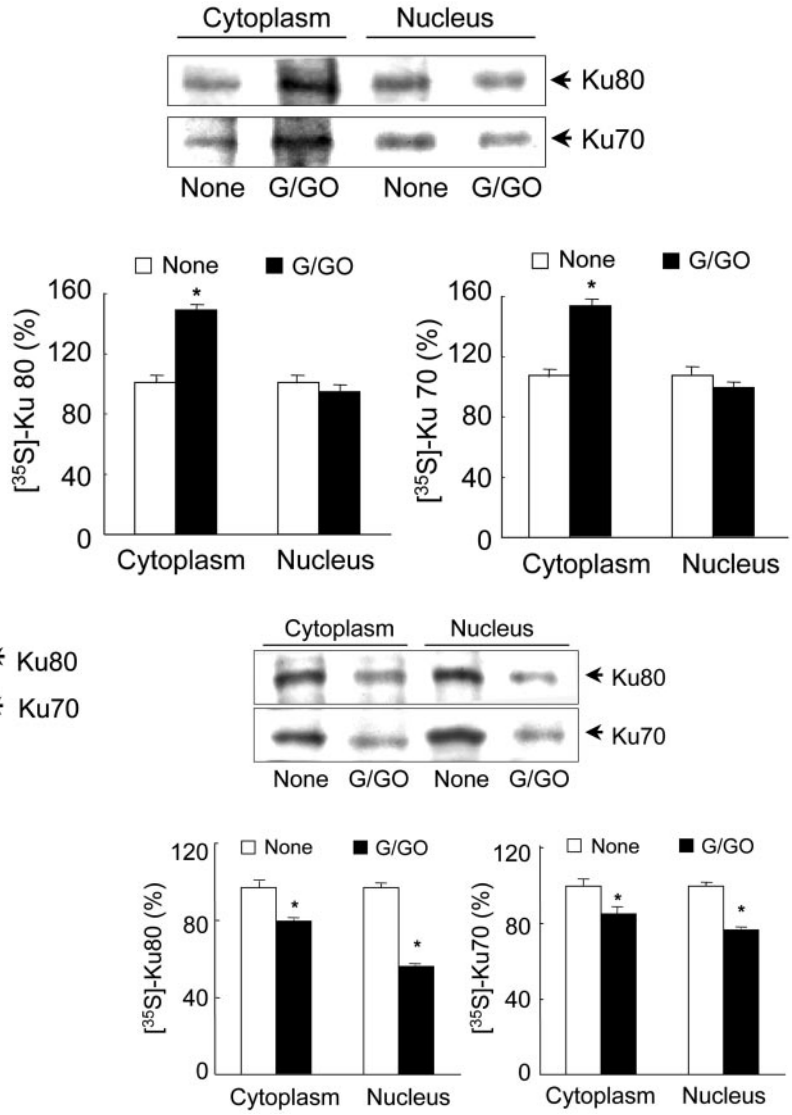

FIG. 10. **Effect of G/GO on Ku synthesis in the cytoplasmic extracts and the nuclear extracts of AR42J cells.** For the pulse experiment, the wild-type cells were treated with or without G/GO and pulsed with [^{35}S]methionine during the last 4 h of each incubation. The density of the cytoplasmic and nuclear extracts from the cells treated without G/GO (*None*) at 12 h was considered to be 100%. The relative densities are expressed as percentages of this value at 12 h. Each *bar* represents the mean ± S.E. of five separate experiments. *, $p < 0.05$ *versus* corresponding to the untreated value. *None*, cells treated without G/GO; *G/GO*, cells treated with G/GO (5 milliunits/ml); *[^{35}S]-Ku80*, [^{35}S]methionine-Ku80; *[^{35}S]-Ku70*, [^{35}S]methionine-Ku70.

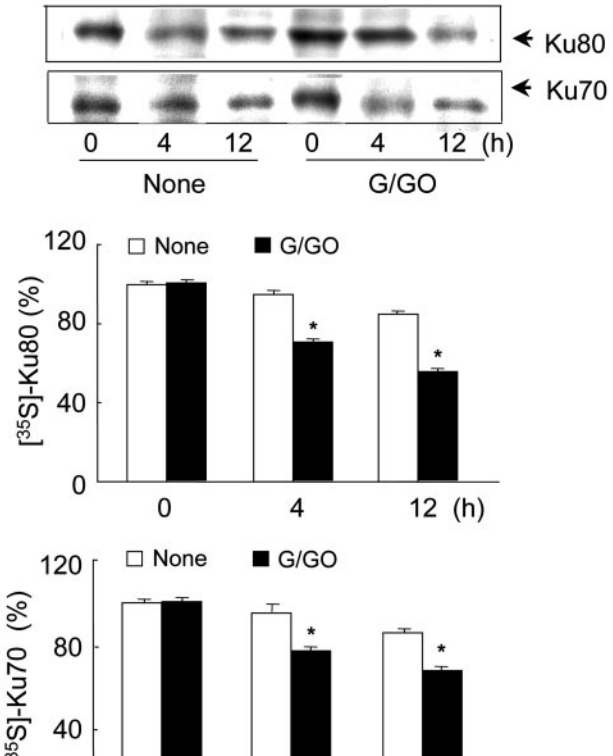

FIG. 11. **Effect of G/GO on Ku degradation in the whole cell extracts of AR42J cells.** For the pulse-chase experiment, the wild-type cells were preincubated with [^{35}S]methionine for 4 h. The cells were then washed with complete DMEM and cultured for 4 and 12 h with or without the G/GO treatment. The density shown in the cells treated without G/GO (*None*) at 0 h was considered as 100%. The relative densities are expressed as percentages of this value at 0 h. Each *bar* represents the mean ± S.E. of five separate experiments. *, $p < 0.05$ *versus* corresponding to the untreated value at each time point (4 or 12 h). *None*, cells treated without G/GO; *G/GO*, cells treated with G/GO (5 milliunits/ml); *[^{35}S]-Ku80*, [^{35}S]methionine-Ku80; *[^{35}S]-Ku70*, [^{35}S]methionine-Ku70.

FIG. 12. **Effect of G/GO on Ku degradation in the cytoplasmic extracts and the nuclear extracts of AR42J cells.** For the pulse-chase experiment, the wild-type cells were preincubated with [^{35}S]methionine for 4 h. The cells were then washed with complete DMEM and cultured for 12 h with or without the G/GO treatment. The density of the cytoplasmic and nuclear extracts from the cells treated without G/GO (*None*) at 12 h was considered to be 100%. The relative densities are expressed as percentages of this value at 12 h. Each *bar* represents the mean ± S.E. of five separate experiments. *, $p < 0.05$ *versus* corresponding to the untreated value. *None*, cells treated without G/GO; *G/GO*, cells treated with G/GO (5 milliunits/ml); *[^{35}S]-Ku80*, [^{35}S]methionine-Ku80; *[^{35}S]-Ku70*, [^{35}S]methionine-Ku70.

extracts and 76.08 ± 1.01 in the nuclear extracts at 12 h of culture.

Effect of G/GO on Ku Binding to Importin α and Importin β as Well as Importin β Level in the Whole Cell Extracts of AR42J Cells—To monitor the changes in the binding of Ku70 and Ku80 to importin α and importin β during G/GO-induced apoptosis, GST and GST-importin-α fusion protein were used. Bound proteins to GST-importin-α fusion protein in the whole cell extracts were detected by Western blot analysis using anti-Ku70, anti-Ku80, and anti-importin β antibodies. Both Ku70 and Ku80 levels in the whole cell extracts were decreased by the G/GO treatment dose-dependently, whereas importin β was not affected by G/GO at 12 h (Fig. 13*A*). There was no protein bound to GST. G/GO had no effect on protein level of importin β in AR42J cells (Fig. 13*B*).

DISCUSSION

The relationship between ROS and apoptosis in the pathophysiology of acute pancreatitis in acinar cells has been re-

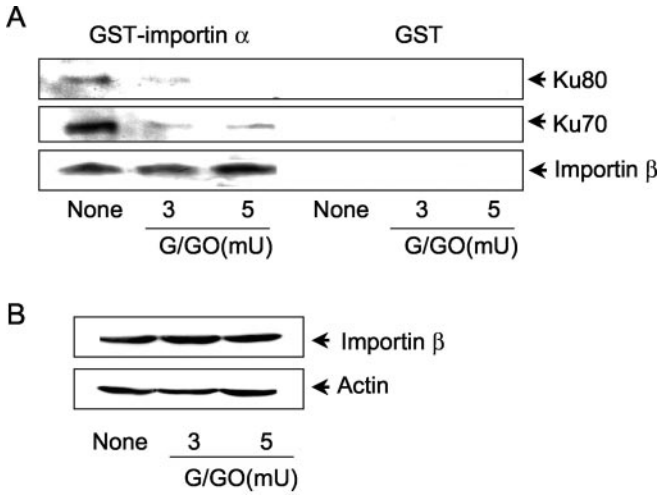

FIG. 13. **Effect of G/GO on Ku binding to importin α and importin β as well as the importin β level in the whole cell extracts of AR42J cells.** To determine the nuclear import of Ku proteins, *in vitro* binding assay using GST or GST-importin α fusion protein was performed in the wild-type cells treated with or without G/GO (3 and 5 milliunits/ml) for 12 h. The bound protein levels were determined by Western blotting for Ku70, Ku80, and importin β (*A*). The importin β level was monitored in the wild-type cells treated with or without G/GO (3 and 5 milliunits/ml) for 12 h (*B*). Actin was used for the protein loading control. The Western result in each lane is the representative of five separate experiments. *None*, cells treated without G/GO.

ported (19, 20). In cerulein-induced pancreatitis, a high degree of ROS generation and apoptosis were observed in pancreatic acinar cells (17, 56, 59). In 38 chronic pancreatitis patients, the distribution of caspase-1 expression was correlated with the extent of apoptosis of acinar cells in pancreatic tissues (61). These studies indicated the possibility that the development of apoptotic cell death caused by ROS may reflect the severity of pancreatitis, which might have substantial clinical value. Elucidating the molecular mechanisms of pancreatic cell death will provide valuable insights into clinical pancreatic disorders and may offer potential pharmacological interventions. The AR42J cell line is the only currently available cell line that maintains many characteristics of normal pancreatic acinar cells, such as the synthesis and secretion of digestive enzymes (62). AR42J cell receptor expression and signal transduction mechanisms parallel those of pancreatic acinar cells (62). Thus, this cell line has been widely used as an *in vitro* model to study cellular secretion, growth, proliferation, and apoptosis of the exocrine pancreas (57, 62–65).

In this study, oxidative stress-induced apoptosis was investigated to determine whether it is related to the low expression level of Ku70 and/or Ku80 in AR42J cells, as determined by the Ku expression level and intracellular distribution, the apoptotic indices (quantification of DNA fragmentation, PARP cleavage, increase in p53 and Bax expression, decrease in Bcl-2 expression), and the Ku-DNA binding activity. Continuous oxidative stress, generated by G/GO, induced apoptotic cell death, which was mediated by low nuclear Ku70 and Ku80 in the cells. Ku70 and Ku80 in the whole cell extracts were not changed by the G/GO treatment. The cytoplasmic Ku80 tended to increase, but the cytoplasmic Ku70 was slightly affected by G/GO. The results clearly demonstrate the novel role of nuclear Ku70 and Ku80 in preventing the apoptosis caused by oxidative stress. The importance of nuclear Ku70 and Ku80 was confirmed by the protection of cell death by the preservation of nuclear Ku70 and Ku80 in the cells transfected with the Ku70 or Ku80 expression gene ($Ku70^+$ and $Ku80^+$) and accelerated cell death by the loss of the Ku-DNA binding activity in the cells transfected with the Ku dominant negative mutant (KuD/N). G/GO-induced decrease in Ku binding to importin α and importin β reflects a possible modification of the nuclear import of Ku70 and Ku80. The importin β level was not changed by G/GO, determined by *in vitro* binding assay using GST-importin α fusion protein and Western blot analysis. These results clearly demonstrated that G/GO did not affect the protein level of nuclear transporter but do affect Ku binding to nuclear transporter importins. G/GO-induced decrease in Ku binding to importins, importin α and importin β, and degradation of Ku70 and Ku80 may cause a loss of defense against oxidative DNA damage, which underlies the mechanism of apoptosis in pancreatic acinar cells.

Oxidative damage to the nucleic acids can produce adducts of the base and sugar residues, which may lead to the generation of single-stranded breaks. Less frequently, oxidation can cause cross-links to other molecules and double-stranded breaks (25). Ischemia/reperfusion in the rabbit spinal cord induces reversible neurological deficits with the increased Ku-DNA binding activity, which is an indicator of DNA-PK activation, whereas severe ischemia/reperfusion causes permanent deficits accompanied by the deceased Ku-DNA binding activity. This suggests that Ku is involved in oxidative injury (26). Fujimura *et al.* (66, 67) recently have reported that a decrease in the DNA base excision repair proteins, apurinic/apyrimidinioc endonuclease and XRCC1, precedes the occurrence of DNA fragmentation after focal cerebral ischemia. Therefore, it is assumed that Ku may play a role in the cell death mechanisms, particularly DNA fragmentation after oxidative stress, and that Ku reduction may involve the mechanism of apoptotic cell death.

Several studies have shown that the inhibition of either Ku70 or Ku80 expression resulted in the induction of apoptosis in human promyelocytic leukemia HL-60 cells and activated human peripheral blood lymphocytes (68), embryonic stem cells and pre-B cells (69), and human HCT116 colon cancer cells (70). In contrast, no loss of the Ku protein was noted in the cells undergoing apoptosis by x-ray irradiation in human glioma cells (71) and in Fas-mediated apoptosis in Jurkat cells (72, 73). This is despite the fact that DNA-PK was cleaved by the caspases during apoptosis in these cells. A DNA-PK deficiency in the cultured neurons caused an accumulation of DNA damage and increased susceptibility to caspase-independent forms of apoptosis (74). Therefore, the exact mechanism by which the selective reduction of Ku occurs during the apoptosis is unclear. Furthermore, there is no consistent evidence as to whether or not the Ku proteins are degraded in the cells under oxidative stress.

There is some evidence suggesting the involvement of caspase-3 activation in H_2O_2-induced apoptosis in HL-60 cells (31, 32), cultured astrocytes (33), activated human peripheral blood lymphocytes (34), hepatoblastoma HepG2 cells (35), and human neuroblastoma cells (36). They suggested H_2O_2 as a second messenger of the death signal in some diseases linked to oxidative stress stimuli. Both cell death and PARP cleavage were prevented either by the caspase-3 inhibitor (31, 34) or a known antioxidant glutathione (35). In contrast, high concentrations of H_2O_2 (above 300 nmol/ml) suppressed both the activation and the activity of the caspases, possibly by modulating the redox status of the cells and the oxidation of the cysteine residues in the caspases. They also showed that low concentration of H_2O_2 (50 nmol/ml) induced apoptosis in Jurkat T-lymphocytes (75). The time points used in this study were 12 h for Ku expression and 24 h for apoptotic cell death. The H_2O_2 produced in the cells treated with G/GO (5 milliunits/ml) was 17.11 nmol/ml at 12 h and 64.03 nmol/ml at 24 h, respectively. Therefore, the H_2O_2-induced apoptosis is supported by these previous studies (31–36, 75). To determine the exact

mechanism responsible for the reduction in the nuclear Ku70 and Ku80 after oxidative stress, Ku expression was observed in the cells treated with G/GO in either the presence or absence of the caspase-3 inhibitor in this study. The reduction in nuclear Ku proteins of the cells undergoing apoptosis was blocked by the treatment with the caspase-3 inhibitor. The caspase-3 inhibitor prevented the loss of nuclear Ku70 and Ku80 in apoptotic cells, determined by Ku expression level and intracellular distribution. These results suggest that the caspase cascade during apoptosis may involve the degradation of Ku70 and Ku80. Therefore, after oxidative stress, the reduction in Ku might be involved in downstream from the caspase-activating apoptotic pathway. There are studies on the subcellular localization of Ku70 and Ku80 (40, 41, 76, 77) demonstrating that the control mechanism for subcellular localization of Ku70 and Ku80 plays a key role in regulating the physiological function of Ku *in vivo*. Each Ku subunit can translocate to the nucleus not only through its own NLS, but also through heterodimerization with each other (78). The Ku70 NLS and the Ku80 NLS are mediated to target to the nuclear rim by two components of the nuclear pore-targeting complex, importin α, and importin β (40, 41). The active nuclear transporter, importin α, has an essential role for the nuclear transport of the apoptotic signaling molecules including the caspases (79). Because Ku70 and the caspases share the same nuclear transporter, Ku70 may be cleaved by the caspases in the nucleus during apoptosis. This possibility is supported by studies showing that activated capase-3 was observed in the nucleus during apoptosis (80), and both the DNA-PKcs and PARP are substrates for caspase-3-like activities after ischemia/reperfusion (26). In addition, the well known nucleoporins Nup153, RanBP2, Nup214, and Tpr, which binds the soluble components of the nuclear transport machinery such as the importin family and the small GTPase Ran (81, 82), are cleaved by caspases during apoptosis (37). Nucleoporin cleavage may affect the nucleocytoplasmic transport in the cells during apoptosis, even though nuclear transport factors, Ran, importin α, and importin β are not proteolytically processed (37). Endoh *et al.* (83) reported the insignificant difference between the total protein levels of Ku70 and Ku80 by x-ray irradiation in rats even though the nuclear translocation of Ku70 and Ku80 from the cytoplasm was inhibited after x-ray irradiation. This led to the inhibition of the fast repair process of DNA double-stranded breaks. The inhibition of the nuclear translocation of the Ku proteins by oxidative stress might be another possible explanation for the loss of nuclear Ku70 and Ku80 and the slight increases in the cytoplasmic Ku proteins in AR42J cells undergoing apoptosis. The results from the pulse experiment and the pulse-chase experiment show that Ku synthesis is increased by oxidative stress, which might result from the homeostasis of the cells because the expressions of both Ku70 and Ku80 were decreased by the G/GO treatment. Moreover, the G/GO-induced loss of Ku70 and Ku80 were shown in both the cytoplasmic and nuclear extracts. These results clearly demonstrate that even though Ku70 and Ku80 were degraded by G/GO in the cytoplasm, the Ku protein levels could be maintained by the newly synthesized Ku proteins by G/GO. Because the Ku binding to the importin family was decreased and nuclear Ku proteins were degraded by oxidative stress in the present study, the significant loss of the nuclear Ku proteins were shown in the cells exposed to oxidative stress, resulting in the loss of defense against oxidative DNA damage and apoptosis in pancreatic acinar cells.

In addition to degradation of Ku proteins by ROS secondarily through caspase activation, ROS may directly contribute to the reduction in the Ku protein and activate another oxidative stress-triggered process. Previous studies show that ROS could reduce the DNA repair activity (84) and directly damage the DNA repair enzyme (25). In the case of severe oxidative DNA damage against DNA repair, the activated p53 protein has been shown to induce apoptosis directly or through the activation of other apoptosis-regulating genes, such as Bax (86, 87). Li *et al.* (70) demonstrated that Ku80 inactivation resulted in the induction of the tumor suppressor protein p53, which contributed to the inhibition of cell growth. Our previous study showed that ROS produced by *Helicobacter pylori* caused p53 and Bax expression and decreased Bcl-2 expression as well as the nuclear loss of Ku70 and Ku80 in human adenocarcinoma AGS cells.[2] These results showed that the nuclear loss of Ku70 and Ku80 was related to the induction of p53 and Bax as well as the decrease in Bcl-2 in the wild-type cells undergoing oxidative stress-mediated apoptosis. In B cell chronic lympocytic leukemia, the level of antiapoptotic Bcl-2 showed a positive correlation with the Ku80 level (88). Both Ku70 and Ku80 expression was higher in aggressive breast tumor compared with that in normal tissue (89), which suggests a possible relationship among the levels of Bcl-2 and Ku70 and Ku80 and anti-apoptosis in some cancer cells. As another subcellular mechanism of apoptosis induced by the oxidative DNA damage, PARP overactivation by severely damaged DNA may trigger apoptosis through excessive energy consumption during DNA repair (60, 90). The possible involvement of anti- and pro-apoptotic molecules on Ku protein expression should be investigated in another study in relation to pancreatic acinar cell death.

It was demonstrated that the inhibition of the Ku-DNA binding activity by the transfection of the C-terminal Ku80 (427–732) expression gene resulted in an increase in apoptotic cell death in AR42J cells. In other reports, Ku80 or Ku70 inactivation diminished the expression of the other Ku subunit (Ku70 or Ku80) and inhibited Ku-DNA binding as well as DNA-PK activity in either Ku70 or Ku80-dificient cells (68–70). From these results, it is postulated that the disruption of either Ku subunit would reduce the Ku-DNA binding activity, which inhibits the functional role of the Ku proteins. Therefore, the induction of apoptosis caused by the reduction in the nuclear level of Ku70 and Ku80 may be related to the loss of the Ku-DNA binding activity. This was proven by the result showing that the inhibition of the Ku-DNA binding activity by the transfection of the C-terminal Ku80 (427–732) resulted in an increase in apoptotic cell death.

In this study, the G/GO-induced decrease in the nuclear Ku70 and Ku80 levels were prevented in both the $Ku70^+$ cells and the $Ku80^+$ cells. However, the prevention against G/GO-induced loss of the nuclear Ku70 and Ku80 were more evident in the $Ku80^+$ cells. The decrease in the number of viable cells and the increase in DNA fragmentation induced by G/GO treatment were inhibited similarly in both the $Ku70^+$ and $Ku80^+$ cells. These results demonstrate that both Ku70 and Ku80 contribute to the stability of the other Ku subunit. Featherstone and Jackson (23) demonstrated the similarities between the Ku70 and Ku80 knockout mice because the two subunits appear to work in a tight complex *in vivo*, and the loss of one subunit of the Ku proteins destabilizes the other. The small amount of Ku80 remaining in the Ku70 knockout cells can promote DNA end joining by working as a monomer or homodimer. In addition to the fact that Ku70 and Ku80 are the primary partners for each other (85), the present results suggest the sparing action of Ku proteins, as one subunit, may stabilize the other subunit under the condition of the loss of one subunit.

[2] J. Y. Song, J. W. Lim, H. Kim, T. Morio, and K. H. Kim, unpublished data.

These results suggest that the oxidative stress-induced apoptosis may be mediated by the activated caspase-3, which degrades the DNA repair protein Ku70 and Ku80, and the decrease in Ku binding to nuclear transporter importin α and importin β, resulting in the reduced nuclear Ku proteins in pancreatic acinar cells. The nuclear loss of Ku70 and Ku80 may cause the loss of the defense against oxidative DNA damage, which underlies the mechanism of apoptotic cell death in pancreatic acinar cells after oxidative stress.

REFERENCES

1. Sanfey, H., Bulkeley, G. B., and Cameron, J. L. (1985) *Ann. Surg.* **201,** 63–69
2. Aho, H. J., Nevalainen, T. J., and Havia, V. T. (1982) *Acta Pathol. Microbiol. Immunol. Scan. A* **90,** 367–373
3. Nonaka, A., Manabe, T., and Tamura, K. (1990) *Nippon Geka Gakkai Zasshi* **2,** 169–173
4. Wisner, J., Green, D., and Ferrell, L. (1988) *Gut* **29,** 1516–1523
5. Guyan, P. M., Udern, S., and Braganza, J. M. (1990) *Free Rad. Biol. Med.* **8,** 347–354
6. Schenberg, M. H., Birk, D., and Berger, H. G. (1995) *Am. J. Clin. Nutr.* **62,** 1306S–1314S
7. Schenberg, M. H., Buchler, M., and Pietrzyk, C. (1995) *Pancreas* **10,** 36–43
8. Schenberg, M. H., Buchler, M., and Berger, H. G. (1988) *Br. J. Surg.* **75,** 1254–1262
9. Scott, P., Bruce, C., and Schofield, D. (1993) *Br. J. Surg.* **80,** 750–754
10. Petrone, W. F., English, D. K., and Wong, K. (1980) *Proc. Natl. Acad. Sci. U. S. A.* **77,** 159–1163
11. Bjork, J., and Arfors, K. E. (1984) *Agents Actions* **11,** 63–73
12. Guice, K. S., Oldham, K. T., and Caty, M. G. (1989) *Ann. Surgery* **210,** 740–747
13. Cohen, M. C., and Cohen, S. (1996) *Am. J. Clin. Pathol.* **105,** 589–598
14. Balkwill, F. R., and Burke, F. (1996) *Immunol. Today* **10,** 299–303
15. Gukovskaya, A. S., Perkins, P., Zaninovic, V., Sandoval, D., Rutherford, R., Fitzsimmons, T., Pandol, S. J., and Poucell-Hatton, S. (1996) *Gastroenterology* **110,** 875–884
16. Kaiser, A. M., Saluja, A. K., Lu, L., Yamanaka, K., Yamaguchi, Y., and Steer, M. L. (1996) *Am. J. Physiol.* **271,** C982–C993
17. Gukovskaya, A. S., Gukovsky, I., Zaninovic, V., Song, M., Sandoval, D., Gukovsky, S., and Pandol, S. J. (1997) *J. Clin. Invest.* **100,** 1853–1862
18. Kaiser, A. M., Saluja, A. K., Sengupa, A., Saluja, M., and Steer, M. L. (1995) *Am. J. Physiol.* **269,** C1295–C1304
19. Kerr, J. F. R., Wyllie, A. H., and Currie, A. R. (1972) *Br. J. Cancer* **26,** 239–245
20. Carson, D. A., and Ribeiro, J. M. (1993) *Lancet* **341,** 1251–1254
21. Kaiser, A. M., Saluja, A. K., Sengupta, A., Saluja, M., and Steer, M. L. (1995) *Am. J. Physiol.* **269,** C1295–C1304
22. Sandoval, D., Gukovskaya, A., Reavey, P., Gukovsky, S., Sisk, A., Braquet, P., Pandol, S. J., and Poucell-Hatton, S. (1996) *Gastroenterology* **111,** 1081–1091
23. Featherstone, C., and Jackson, S. P. (1999) *Mutat. Res.* **434,** 3–15
24. Bliss, T. M., and Lane, D. P. (1997) *J. Biol. Chem.* **272,** 5765–5773
25. Beckman, K. B., and Ames, B. N. (1998) *Physiol. Rev.* **78,** 547–581
26. Shackelford, D. A., Tobaru, T., Zhang, S., and Zivin, J. A. (1999) *J. Neurosci.* **19,** 4727–4738
27. Arrington, E. D., Caldwell, M. C., Kumaravel. T. S., Lohani, A., Joshi, A., Evans, M. K., Chen, H. T., Nussenzweig, A., Holbrook, N., and Gorospe, M. (2000) *Free Rad. Biol. Med.* **29,** 1166–1176
28. Buttke, T. M., and Sandstrom, P. A. (1994) *Immunol. Today* **15,** 7–10
29. Nicholson, D. W., and Thornberry, N. A. (1997) *Trend Biochem. Sci.* **22,** 299–306
30. Chandra, J., Samali, A., and Orrenus, S. (2000) *Free Rad. Biol. Med.* **29,** 323–333
31. Matsura, T., Kai, M., Fujii, Y., Ito, H., and Yamada, K. (1999) *Free Rad. Res.* **30,** 73–83
32. Mizutani, H., Tada-Oikawa, S., Hiraku, Y., Oikawa, S., Koijima M, and Kawanishi S. (2002) *J. Biol. Chem.* **277,** 30684–30689
33. Takuma, K., Mori, K., Lee, E., Enomoto, R., Baba, A., and Marsuda, T. (2002) *Brain Res.* **946,** 232–238
34. Velez-pardo, C., Ospina, G. G., and Jimenez del Rio, M. (2002) *Neurotoxicol.* **23,** 351–365
35. Emanuele, S., Calvaruso, G., Lauricella, M., Giuliano, M., Bellavia, G., D'Anneo, A., Vento, R., and Tesoriere, G. (2002) *Int. J. Oncol.* **21,** 857–865
36. Jang, M. H., Lee, T. H., Shin, M. C., Bahn, G. H., Kim, J. W., Shin, D. H., Kim, E. H., and Kim, C. J. (2002) *Neurosci. Lett.* **329,** 177–180
37. Ferrando-May, E., Cordes, V., Biller-Ckovric, I., Mirkovic, J., Gorlich, D., and Nicotera, P. (2001) *Cell Death Differ.* **8,** 495–505
38. Ohno, M., Fornerod, M., and Mattaj, I. W. (1998) *Cell* **92,** 327–336
39. Dingwall, C., and Laskey, R. A. (1991) *Trends Biol. Sci.* **16,** 478–481
40. Koike, M., Awaji, T., Kataoka, M., Tsujimoto, G., Kartasova, T., Koike, A., and Shiomi, T. (1999) *J. Cell Sci.* **112,** 4031–4039
41. Koike, M., Ikuta, T., Miyasaka, T., and Shiomi, T. (1999) *Oncogene* **18,** 7495–7505
42. Marangoni, E., Foray, N., O'Driscoll, M., Douc-Rasy, S., Bernier, J., Bourhis, J., and Jeggo, P. (2000) *Nucleic Acids Res.* **28,** 4778–4782
43. Thurman, R. G., Ley, H. G., and Scholz, R. (1972) *Eur. J. Biochem.* **25,** 420–430
44. Kim, S. H., Kim, D., Han, J. S., Jeong, C. S., Chung, B. S., Kang, C. D., and Li, G. C. (1999) *Cancer Res.* **59,** 4012–4017
45. Lim, J. W., Kim, H., and Kim, K. H. (2002) *J. Biol. Chem.* **277,** 46093–46100
46. Bradford, M. M. (1976) *Anal. Biochem.* **72,** 248–254
47. Li, J. J., Westergaard, C., Ghosh, P., and Colburn, N. H. (1997) *Cancer Res.* **57,** 3569–3576
48. Xu, Y., Bialik, S., Jones, B. E., Limuro, Y., Kitsis, R. N., Srinivasan, A., Brenner, D. A., and Czaja, M. J. (1998) *Am. J. Physiol.* **275,** C1058–C1066
49. Reeves, W. H. (1992) *Rheum. Dis. Clin. North Am.* **18,** 391–414
50. Holstein, S. A., Wohlford-Lenane, C. L., and Hohl, R. J. (2002) *J. Biol. Chem.* **277,** 10678–10682
51. Xie, Y., Skytting, B., Nilsson, G., Gasbarri, A., Haslam, K., Bartolazzi, A., Brodin, B., Mandahl, N., and Larsson, O. (2002) *Cancer Res.* **62,** 3861–3867
52. Frangioni, J. V., and Neel, B. G. (1993) *Anal. Biochem.* **210,** 179–187
53. Tallarida, R. J., and Murray, R. B. (1987) *Manual of Pharmacological Calculations with Computer Programs*, pp. 121–125, Springer-Verlag New York, Inc., New York
54. Hiraishi, H., Terano, A., and Ota, S. (1991) *Am. J. Physiol.* **261,** G921–G928
55. Harlan, J. M., Levine, J. D., Callahan, K. S., and Schwarz, B. R. (1984) *J. Clin. Invest.* **73,** 706–713
56. Yu, J. H., Lim, J. W., Namkung, W., Kim, H., and Kim, K. H. (2002) *Lab. Inv.* **82,** 1359–1368
57. Piiper, A., Leser, J., Lutz, M. P., Beil, M., and Zenzem, S. (2001) *Biochem. Biophys. Res. Commun.* **287,** 746–751
58. Nicke, B., Tseng, M. J., Fenrich, M., and Logsdon, C. D. (1999) *Am. J. Physiol.* **276,** G499–G506
59. Kimura, K., Shimosegawa, T., Sasano, H., Abe, R., Satoh, A., Masamune, A., Koizumi, M., Nagura, H., and Toyota, T. (1998) *Gastroenterology* **114,** 372–381
60. Endres, M., Wang, Z. Q., Namura, S., Waeber, C., and Moskowitz, M. A. (1997) *J. Cereb. Blood Flow Metab.* **17,** 1143–1151
61. Ramadani, M., Yang, Y., Gansauge, F., Gansauge, S., and Beger, H. G. (2001) *Pancreas* **22,** 383–387
62. Christophe, J. (1994) *Am. J. Physiol.* **266,** G963–G971
63. Scemama, J. L., Fourmy, D., Zahidi, A., Pradayrol, L., Susini, C., and Ribet, A. (1987) *Gut* **28,** 233–236
64. Sata, N., Klonowski-Stumpe, H., Han, B., Luthen, R., Haussinger, D., and Niederau, C. (1997) *Pancreas* **15,** 278–284
65. Masamune, A., Sasaki, Y., Satoh, A., Fujita, M., Yoshida, M., and Shimosegawa, T. (2001) *Pancreas* **22,** 75–83
66. Fujimura, M., Morita-Fujimura, Y., Kawase, M., and Chan, P. H. (1999) *J. Cereb. Blood Flow Metab.* **19,** 495–501
67. Fujimura, M., Morita-Fujimura, Y., Sugawara, T., and Chan, P. H. (1999) *Stroke* **30,** 2456–2462
68. Ajmani, A. K., Satoh, M., Reap, E., Cohen, P. L., and Reeves, W. H. (1995) *J. Exp. Med.* **181,** 2049–2058
69. Nussenzweig, A., Sokol, K., Burgman, P., Li, L., and Li, G. C. (1997) *Proc. Natl. Acad. Sci. U. S. A.* **94,** 13588–13593
70. Li, G., Nelsen, C., and Hendrickson, E. A. (2002) *Proc. Natl. Acad. Sci. U. S. A.* **99,** 832–837
71. Song, Q., Lees-Miller, S. P., Kumar, S., Zhang, Z., Chan, D. W., Smith, G. C., Jackson, S. P., Alnermri, E. S., Litwack, G., Khanna, K. K., and Lavin, M. F. (1996) *EMBO J.* **15,** 3238–3246
72. Teraoka, H., Yumoto, Y., Yatanabe, F., Tsukada, K., Suwa, A., Enari, M., and Nagata, S. (1996) *FEBS Lett.* **393,** 1–6
73. McConnell, K. R., Dynan, W. S., and Hardin, J. A. (1997) *J. Immunol.* **158,** 2083–2089
74. Chechlacz, M., Vemuri, M. C., and Naegele, J. R. (2001) *J. Neurochem.* **78,** 141–154
75. Hampton, M. B., and Orrenius, S. (1997) *FEBS Lett.* **414,** 552–556
76. Teoh, G., Urashima, M., Greenfield, E. A., Nguyen, K. A., Lee, J. F., Chauhan, D., Ogata, A., Treon, S. P., and Anderson, K. C. (1998) *J. Clin. Invest.* **101,** 1379–1383
77. Morio, T., Hanissian, S. H., Bacharier, L. B., Teraoka, H., Nonoyama, S., Seki, M., Kondo, J., Nakano, H., Lee, S. K., Geha, R. S., and Yata, J. (1999) *Immunity* **11,** 339–348
78. Koike, M., Shiomi, T., and Koike, A. (1999) *Exp. Cell Res.* **250,** 401–413
79. Yashuhara, N., Eguchi, Y., Tachibana, T., Imamoto, N., Yoneda, Y., and Tsujimoto, Y. (1997) *Genes Cells* **2,** 55–64
80. Mandal, M., Adam, L., and Kumar, R. (1999) *Biochem. Biophys. Res. Commun.* **260,** 775–780
81. Saitoh, H., Cooke, C. A., Burgess, W. H., Earnshaw, W. C., and Dasso, M. (1996) *Mol. Biol. Cell* **7,** 1319–1334
82. Nakielny, S., Shaikh, S., Burke, B., and Dreyfuss, G. (1999) *EMBO J.* **18,** 1982–1995
83. Endoh, D., Okui, T., Kon, Y., and Hayshi, M. (2001) *Radiat. Res.* **155,** 320–327
84. Hu, J. J., Dubin, N., Kurland, D., Ma, B. L., and Roush, G. C. (1995) *Mutat. Res.* **336,** 193–201
85. Osipovich, O., Durum, S. K., and Muegge, K. (1997) *J. Biol. Chem.* **272,** 27259–27265
86. Miyashita, T., and Reed, J. C. (1995) *Cell* **80,** 293–299
87. Tamura, T., Ishihara, M., Lamphier, M. S., Tanaka, N., Oishi, I., Aizawa, S., Matsuyama, T., Mak, T. W., Taki, S., and Taniguchi, T. (1995) *Nature* **376,** 596–599
88. Klein, A., Miera, O., Bauer, O., Golfier, S., and Schriever, F. (2000) *Leukemia* **14,** 40–46
89. Pucci, S., Mazzarelli, P., Rabitti, C., Giai, M., Gallucci, M., Flammia, G., Alcini, A., Altomare, V., and Fazio, V. M. (2001) *Oncogene* **20,** 739–747
90. Szab, C., Zingarelli, B., O'Connor, M., and Salzman, A. L. (1996) *Proc. Natl. Acad. Sci. U. S. A.* **93,** 1753–1758